

UNIVERSITY OF  
CAMBRIDGE



*Nucifer*

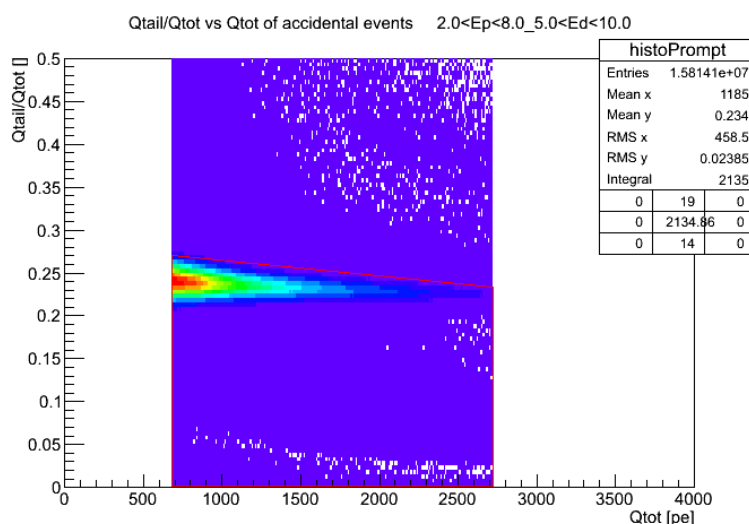


energie atomique • energies alternatives

## End of Part IA Natural Sciences Internship

From 19/08/2013 to 27/09/2013

# Data Analysis for the Nucifer Antineutrino Detection Experiment



Trang-Anh E. NGHIEM

Academic Tutor: Ms. Sylvana TOMASELLI

Natural Sciences, Class of 2012, St John's College, Cambridge

Professional Tutor: Dr. David LHUILLIER



## Special Thanks

I would like to thank Dr. Heloise GOUTTE, head of the SPhN, for welcoming me in her service for my end of IA Natural Sciences research internship.

Special thanks to Dr. David LHUILLIER, my internship tutor, who was always available to answer my questions, give detailed and constructive feedback, discuss results and possible developments despite his very high responsibilities. He gave me a unique opportunity to discover and contribute to multiple aspects in his field of research, while always showing openness, friendliness and encouragement.

Many thanks as well to other members of the Nucifer team, including Dr. Thierry LASSERRE, Dr. Guillaume MENTION, Dr. Vincent FISCHER or Yo KATO, and the SPhN service, including Dr. Nicole D'HOSE, Dr. Pierre GUICHON or Dr. Jaume CARBONELL, for allowing me to feel part of the group and the project despite the short duration of my internship. In particular, I would like to thank Maxime PEQUIGNOT, Dr. Jonathan GAFFIOT and Antoine COLLIN for their very valuable support and advice in programming. My thanks also go to Dr. Heloise GOUTTE and Dr. Michel GARCON for their introduction to their respective research areas.

Last but not least, I present my thanks to my academic tutor Miss Sylvana TOMASELLI without whom this uplifting experience would have been impossible, without forgetting her secretary Miss Jo ASH and the IRFU secretary Mrs Shirley CHIMOT for completing all the administrative work necessary for the derogation application and the internship agreement redaction.

# Contents

A) About the CEA.....	5
B) The Nucifer experiment.....	6
I- Scientific Background .....	6
a) The electronic antineutrino in the Standard Model .....	6
b) Nuclear reactors and non-proliferation .....	7
II- Goals and description .....	8
a) Goals of the Nucifer experiment .....	8
b) Description of the experiment.....	10
C) Internship work.....	15
I- Optimisation of energy and time cuts .....	15
II- Optimisation of the PSD cut.....	18
a) Shape of the plots vs $Q_{tail}/Q_{tot}$ vs $Q_{tot}$ and of the PSD cut .....	20
b) Analysis and optimisation with accidental reactor-on events .....	21
c) Summary of results with all new cuts .....	24
III- Analysis of the ${}^9\text{Li}$ background.....	25
a) How the ${}^9\text{Li}$ question first arose, or ‘The Bump’ .....	25
b) Estimation the number of ${}^9\text{Li}$ events in Nucifer from extrapolation of DC data .....	28
D) Conclusions .....	35
E) References .....	36
F) Appendix.....	37
Appendix 1: Macro examples.....	37
Appendix 2: Error propagation.....	50

## A) About the CEA



View of the CEA Saclay Centre

The Commissariat à l'Energie Atomique et aux Energies Alternatives (CEA) is a government-funded technological research organisation that contributes to 3 main fields: energy, information and health technologies, defense and safety, based on a state-of-the-art fundamental research. Its results are used by the nuclear, energetic and high tech industries in France.

Its head office is located at the Saclay Centre, 91191 Gif-sur-Yvette Cedex.

Here is a list of some of the main events of its history:

- creation in 1945 just after the Second World War
- creation of the Saclay Centre in 1947
- first nuclear reactor and first particle accelerator in 1952
- first French Tokamak in 1973
- first French scanner in 1976
- first research centre for solar energy in 1989
- research on DNA from 1998
- creation of Neurospin in 2006

The CEA has 16,000 employees and 1.500 PhD students over 10 research centres in France, the largest one being the Saclay Centre. It is the 2nd largest patent registrant in France.

It delivers a service at a national level. Its tutor authority is the French Ministry of Industry and Research. It also plays a role at the international scale in the field of the control of nuclear proliferation and of public safety.

The weekly worked time is 40 hours. Employees are allowed 28 vacation days, to which working time compensation days are added.

Because of its very diverse activity fields, the CEA shows a vast range of different professions: researchers, engineers, technicians, computer engineers, librarians, managers, human resources, medical, legal, communication, safety or security professions... The recruitment is directly done at the level of services and laboratories.

## B) The Nucifer experiment

I worked on the Nucifer experiment, a short-range antineutrino detector recording the emissions from the nuclear reactor Osiris. The project has both an application in non-proliferation and potentially substantial implications in fundamental physics.

### I- Scientific Background

#### a) The electronic antineutrino in the Standard Model

mass →	≈2.3 MeV/c <sup>2</sup>	≈1.275 GeV/c <sup>2</sup>	≈173.07 GeV/c <sup>2</sup>	0	≈126 GeV/c <sup>2</sup>
charge →	2/3	2/3	2/3	0	0
spin →	1/2	1/2	1/2	1	0
	<b>u</b> up	<b>c</b> charm	<b>t</b> top	<b>g</b> gluon	<b>H</b> Higgs boson
<b>QUARKS</b>	≈4.8 MeV/c <sup>2</sup> -1/3 1/2 <b>d</b> down	≈95 MeV/c <sup>2</sup> -1/3 1/2 <b>s</b> strange	≈4.18 GeV/c <sup>2</sup> -1/3 1/2 <b>b</b> bottom	0 0 1 <b>γ</b> photon	
	0.511 MeV/c <sup>2</sup> -1 1/2 <b>e</b> electron	105.7 MeV/c <sup>2</sup> -1 1/2 <b>μ</b> muon	1.777 GeV/c <sup>2</sup> -1 1/2 <b>τ</b> tau	91.2 GeV/c <sup>2</sup> 0 1 <b>Z</b> Z boson	<b>GAUGE BOSONS</b>
<b>LEPTONS</b>	<2.2 eV/c <sup>2</sup> 0 1/2 <b>ν<sub>e</sub></b> electron neutrino	<0.17 MeV/c <sup>2</sup> 0 1/2 <b>ν<sub>μ</sub></b> muon neutrino	<15.5 MeV/c <sup>2</sup> 0 1/2 <b>ν<sub>τ</sub></b> tau neutrino	80.4 GeV/c <sup>2</sup> ±1 1 <b>W</b> W boson	
The Standard Model					

The Standard Model of particle physics is a theory that aims at unifying the strong, weak and electromagnetic interactions and describing their effect on the subatomic elementary particles.

The 6 charged quarks are paired up, according to the symmetry of fundamental interactions. Quarks are the constituents of protons and neutrons.

$$p^+ = 2u + d$$

$$n = u + 2d$$

With the electron (lepton), they make up the known matter. The electronic antineutrino, a charge-less and massive lepton, does not form a part of matter, but it is emitted in the quarks u to d or d to u reactions.

The bosons are messengers, or forces. Both the photon and the gluon are massless. The photon, which

has no charge and an infinite range, mediates the electromagnetic interaction. The gluon, which can interact with itself, mediates the strong interaction. By contrast the Z and W bosons have the mass of a Au atom and therefore a very short range of the order of magnitude of  $10^{-18}$  m. They mediate the weak interaction. Quarks are sensitive to all Gauge bosons.

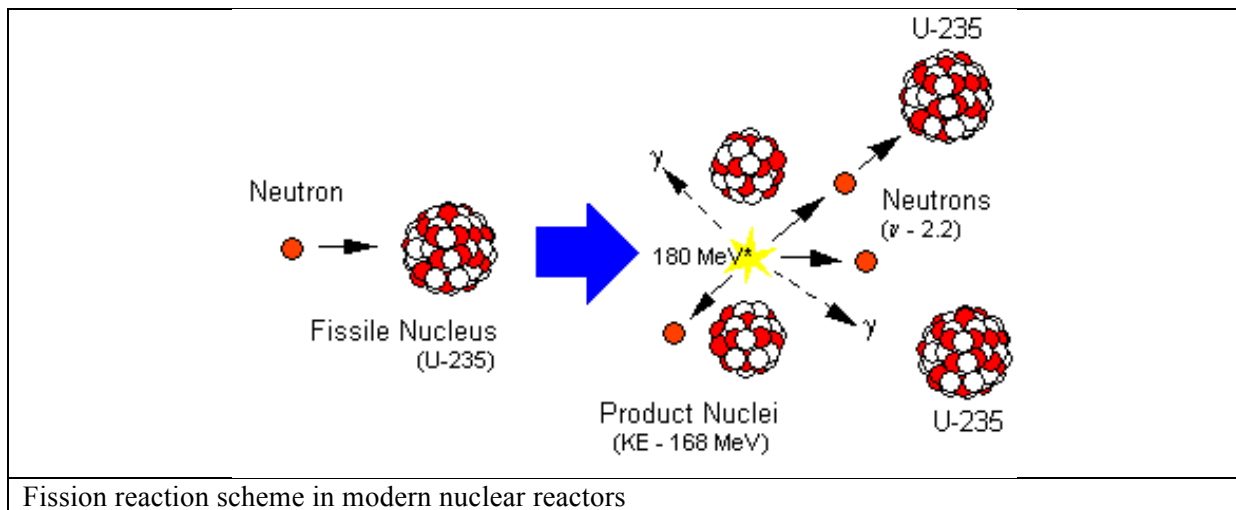
All reactions must conserve the symmetries of all interactions, as well as the leptonic number. The  $\beta$ -reaction that leads to the formation of the electronic antineutrino, in terms of elementary particles, is:

Symmetries	$d$	$\rightarrow$	$u$	+	$e^-$	+	$\bar{\nu}_e$
Electromagnetic	-1/3		+2/3		-1		0
Strong	-		-		-		-
Leptonic number	0		0		+1		-1

This reaction being notoriously hard to detect, the need arises to study it using a very intense source. A typical example is a nuclear reactor.

### b) Nuclear reactors and non-proliferation

Modern nuclear reactors use fissile  $^{235}\text{U}$ . This nucleus has an excess number of neutrons compared to its number of protons, so it becomes more stable ie releases energy when it converts a neutron into a proton, following the reaction scheme above. Each fission produces on average 6 antineutrinos, and 1 GWe of energy released is equivalent to  $10^2$  antineutrinos/s, which gives us large chances to detect them.



Fission is explosive by nature, as a neutron reacting with a fissile nucleus releases 3 neutrons that will in turn react with other nuclei. In reactors, the reaction is controlled thanks to ‘consumable poisons’ such as Gadolinium bars.

$^{235}\text{U}$ , the most widely used combustible in nuclear reactors, may also be used in nuclear weapons. However, it requires centrifugation to be separated from the naturally abundant  $^{238}\text{U}$ .  $^{239}\text{Pu}$ , that is formed in reactors from  $^{235}\text{U}$ , is also fissile and therefore another potential nuclear weapon combustible. As Pu is chemically different from U, it is easier to separate it from the fissile mixture through chemical processes.

During an energy production cycle, the number of neutrinos emitted gradually decreases because, for the same electric power,  $^{239}\text{Pu}$  releases less neutrinos than  $^{238}\text{U}$ . Thus if the reactor is stopped before

the end of the cycle to remove the  $^{239}\text{Pu}$  for military uses, this will result in a discontinuity in the number of neutrinos produced by the reactor.

Therefore, continuously controlling the evolution of the neutrino emission rate throughout the cycle could allow the detection of any tentative of military usage. Neutrino detection presents main advantages as means of reactor control: it is non-intrusive, non-screenable by nature and very difficultly perturbable [1].

## **II- Goals and description**

### **a) Goals of the Nucifer experiment**

#### **i- Application to non-proliferation**

The Nucifer project was started after a demand from the International Atomic Energy Agency (IAEA). The aim is to produce an operational neutrino detector that should:

- be installed without a major impact on the site of an existing nuclear reactor,
- be operable from a distance and require minimal maintenance,
- have its safety inspected and approved by national control authorities,
- present relatively little cost and use a maximum of products available on the market, for possible future serial production [2].

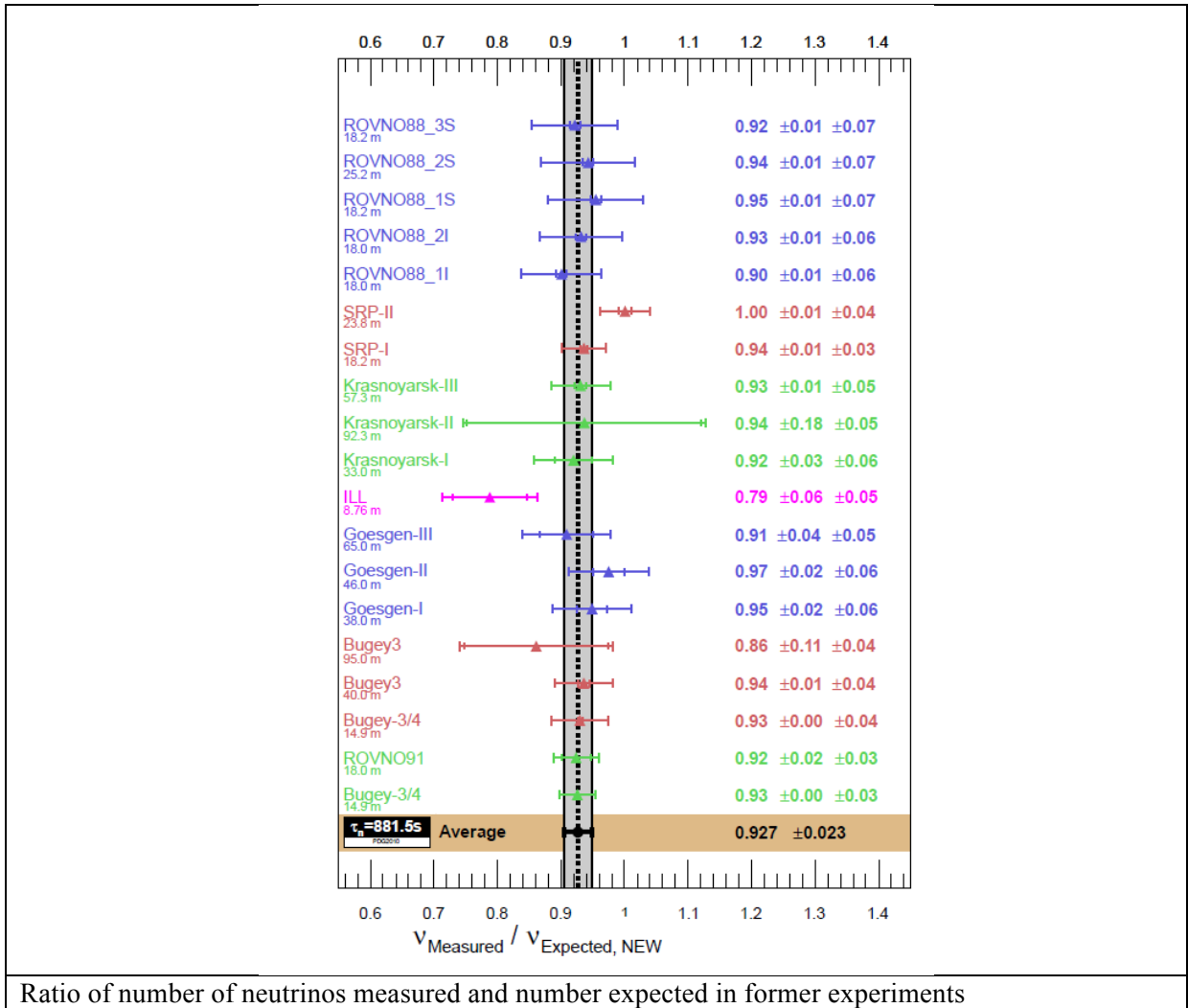
#### **ii- Fundamental scope**

Because neutrinos bear no charges and the wavefunctions of their  $e$ ,  $\mu$  and  $\tau$  flavours overlap, the mixing of the 3 neutrino flavours is possible. The oscillation of neutrinos from a flavour to another actually follows a predictable sinusoidal behaviour, characterised by the mass differences between them and the constant mixture angles between every 2 flavours. The probability of mixture  $P$  at the detector is related to the distance  $L$  to the source and energy  $E$  of the neutrinos, as shown in the equation below. The mass difference  $\Delta m$  between the two antineutrinos and the mixing angle  $\theta$  are characteristics of the particles.

$$P(\overline{\nu}_e \rightarrow \overline{\nu}_\tau) \approx 1 - \sin^2(2\theta_{13}) \sin\left(\frac{\Delta m_{31}^2 L}{4E}\right)$$

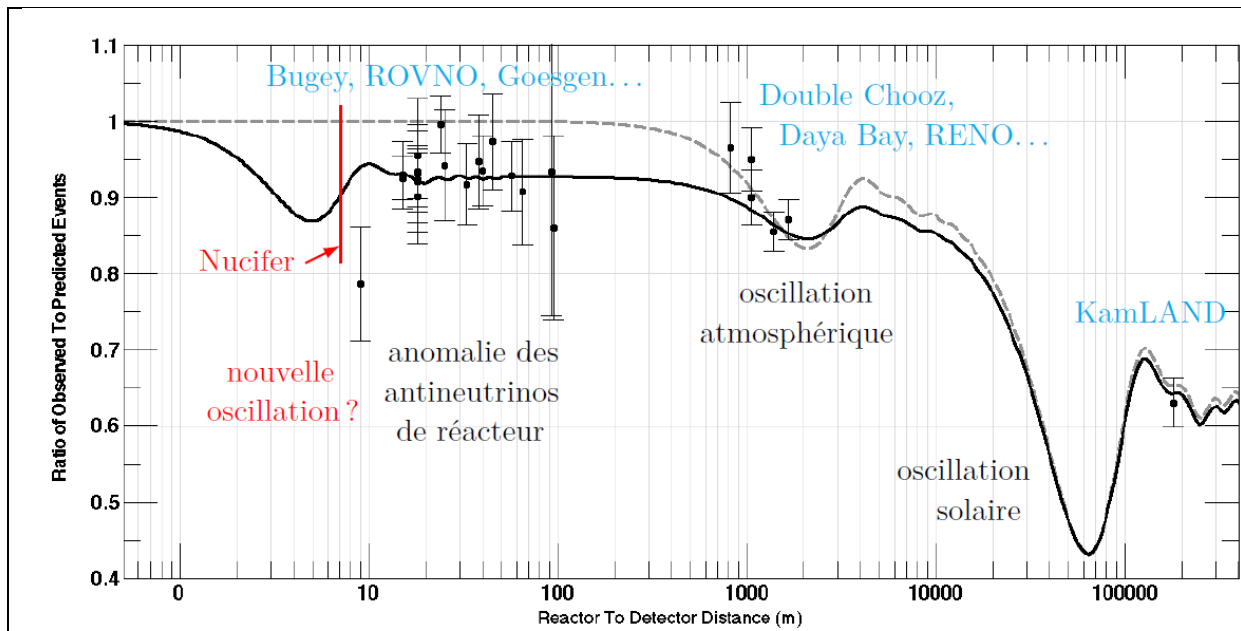
As only electronic antineutrinos can be detected,  $P$  can only be deduced from the deficit of antineutrinos at the detector. However, in many recent experiments, the measured deficit was greater than expected from simulations, such that the number of neutrinos detected was by 7% (ie 3 standard deviations) smaller than the predicted value.





This anomaly, known as the reactor antineutrino anomaly, would be consistent with the existence of a fourth neutrino also called 'sterile neutrino'. This neutrino would have a shorter-period oscillation, and would not interact via fundamental interactions of the Standard Model other than gravitational. The theory predicts no paired antiparticle to the 'sterile neutrino' and a potentially important mass. Prospective answers to the questions of dark matter and of the asymmetry between matter and antimatter might arise from the measured anomaly.

As the distance between Nucifer and the reactor core is too short for any notable oscillations to take place (see figure hereafter), the neutrino deficit should be relatively small, so that a potential oscillation from the fourth neutrino might possibly become observable.

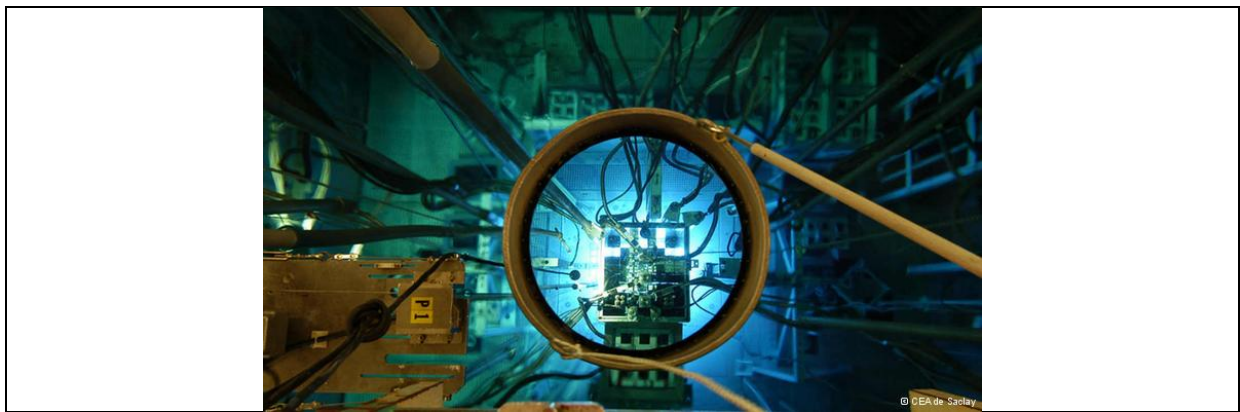


Ratio of Observed to Predicted Events as a function of reactor to detector distance as measured in previous experiments [2] The location of Nucifer is shown in red.

### b) Description of the experiment

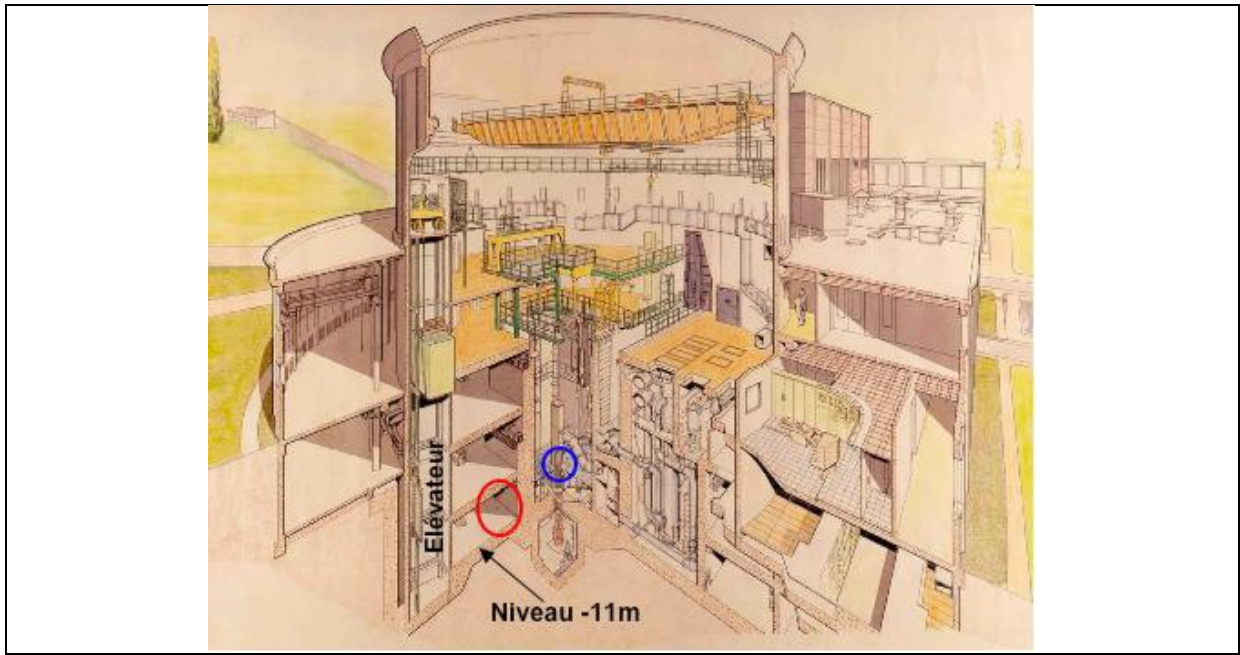
(From here onwards electronic antineutrinos may be called neutrinos for conciseness.)

#### i- Location and apparatus



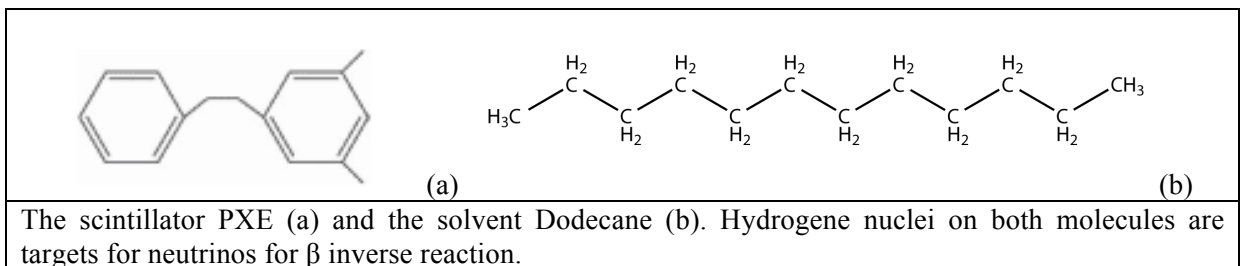
View over the Osiris reactor's open core and water pool

The Nucifer detector is deployed at the Osiris experimental reactor on the CEA Saclay centre (see figure above). The reactor of a maximal power of 70 MW is used primarily to provide a powerful neutronic irradiation for various experimental settings. It also produces medical isotopes and dopes silicium by neutron capture for microelectronics. It is a pool reactor, where the core is cooled and the outside is protected from neutrons or gamma rays escaping from the fission reaction by a pool of pure water. The surface of the pool is in direct contact with the air.

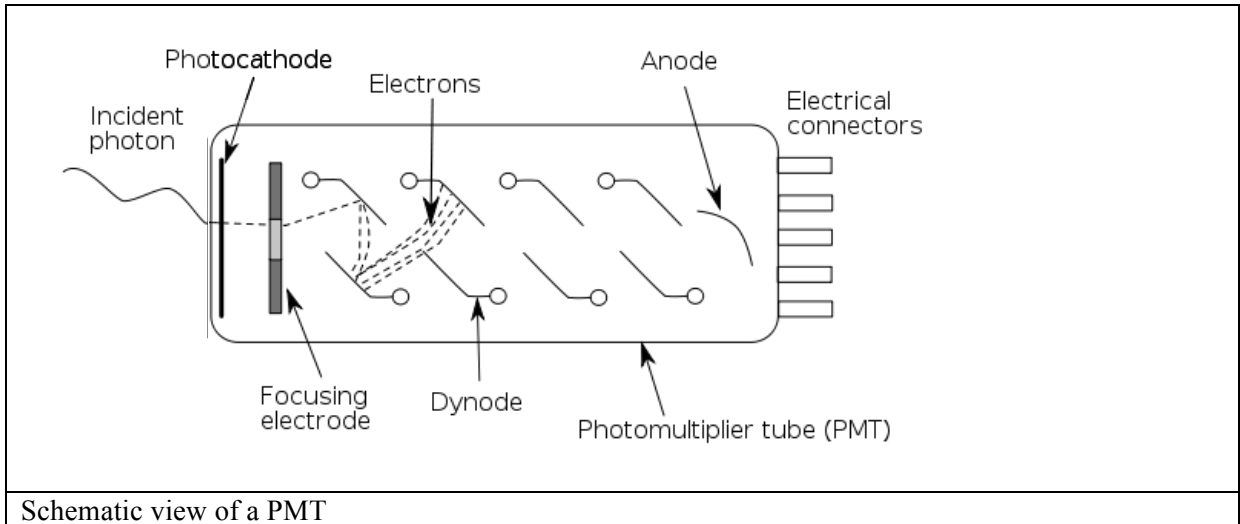


Nucifer at Osiris. The reactor core is circled in blue and Nucifer's location in red.

Nucifer is located 11 m below the pool surface as shown in the figure above. It is only 7m away from the reactor core. The detector itself is cylindrical with 60 cm radius and 73 cm height. It is filled with an organic aromatic scintillating liquid composed of 50 weight per cent (wt%) Phenylxylylethane (PXE) and 50wt% Dodecane (chemical structures in figure below). The scintillating liquid serves both as a target and as a scintillator. Antineutrinos react with the numerous protons on the organic chains, which allows their identification by the detection of the outcomes of the reaction. The scintillation is due to the excitation of the aromatic cycles to higher, unoccupied levels of energy from the energy released by the reaction. As the scintillator molecule relaxes to its initial stable level of energy, it emits the energy difference in the form of photon.

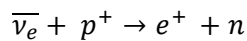


The luminous signal is detected thanks to the 15 photomultiplier tubes (PMT's), vacuum glass bulbs on the detector's top surface. Under the impulsion of a photon, an electron is ripped off the photocathode. Its electric field accelerates the electron towards the first dynode, which is charged with a positive voltage. As the electron strikes the dynode, low energy electrons are emitted. All electrons move towards the next dynode. Each dynode being charged at a more positive voltage than the precedent one, the number of electrons is amplified at each dynode, so that it becomes electronically measurable ad the electrons reach the anode (see diagram hereafter). The amplification factor (the PMT gain) is proportional to the initial photon energy and has a power law dependence on the dynode voltage.



**ii- Detection method**

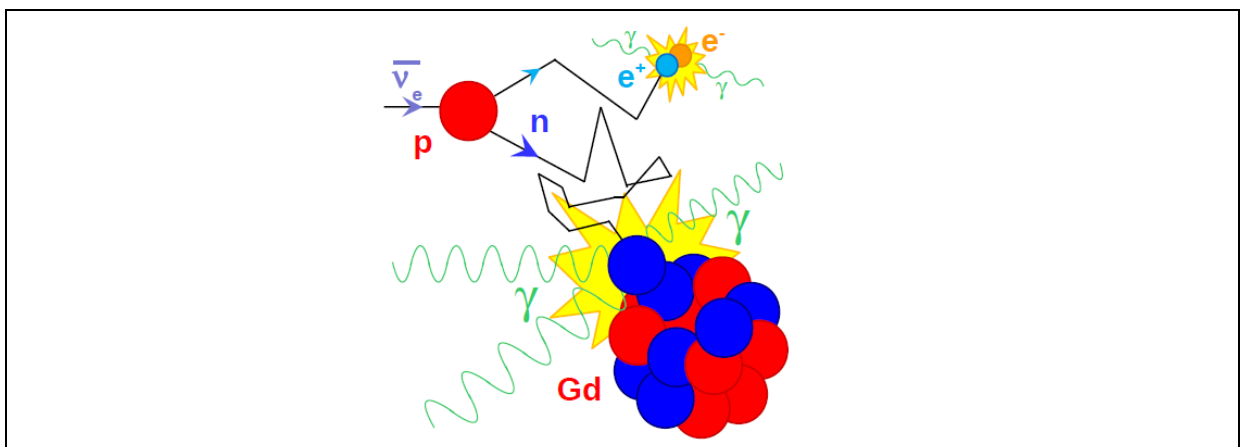
Neutrinos are detected via the inverse Beta reaction [1]:



The mass on the RHS is more important than that on the LHS, therefore an energy input is necessary for the reaction to happen. From the difference between the initial and final masses, it can be determined that the threshold energy of the incoming neutrino is of 1.8 MeV.

Most of the neutrino's initial kinetic energy is transferred to the positron, which undergoes mutual annihilation with an electron within the scintillating liquid. This reaction results in a release of energy, that the scintillator molecules convert into a photon's kinetic energy, ie a light signal with an energy above the initial threshold of 1.8 MeV. This makes up the prompt signal.

The neutron emitted from the inverse Beta reaction with a smaller amount of energy travels through the liquid, losing 1/2 of its kinetic energy every time it collides with a proton (approximately as massive) on the scintillator's organic chain. Eventually the neutron thermalises, its energy equalling to the thermal energy of its environment. It is then captured by a Gd atom, which collects neutrons very readily. The capture is followed by the Gd nucleus' rearrangement, which emits a characteristic photon around 8 MeV, the delayed signal. The prompt and delayed are separated by a time interval of approximately 40µs, dominated by the diffusion time of the neutron.

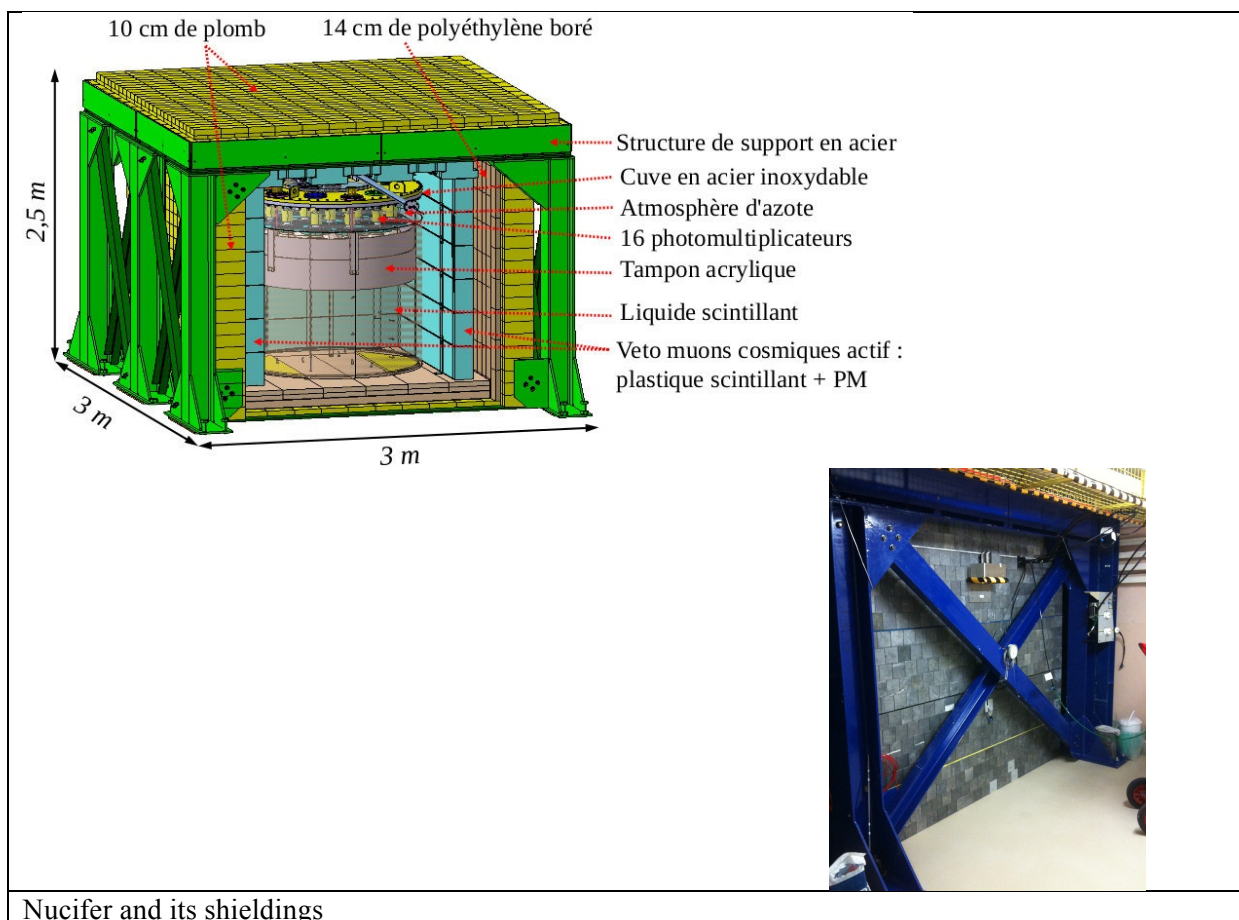


Summary diagram of the neutrino detection mechanism

The correlated prompt and delayed signals, apart by the characteristic time difference, are the signature of the neutrino event. It is therefore important to identify in which energy and time ranges the two signals should be looked for, as well as understand and reject any other source of gamma rays or neutrons.

### iii- Accidental and correlated noise

Identifying the neutrino signal from the noise is the main concern in neutrino detection. In the Nucifer experiment in particular, both the proximity to the core and the very shallow depth underground make the background noise a very important problem. In order to observe a neutrino signal greater than the statistical fluctuation of the background, the shielding and choice of materials for the detector, as well as the rejection of the background and inclusion of the signal in data analysis can be crucial.



Accidental noise refers to aleatory events that independently produce neutrons, gamma rays or any phenomenon that can provoke an ionisation on a scintillating liquid molecule. Cosmic particles that interact in the high atmosphere can create rays of energies varying from ultraviolet to gamma, as well as diverse particles including neutrons themselves or very energetic muons that can release neutrons by spallation. The reactor core, when on, also produces fast neutrons that, despite the 2.25m of water between the core and Nucifer, can reach the scintillator. Natural radioactivity can also contribute through gamma decay, although the most energetic rays, 2.8 MeV from the disintegration of thallium 208, cannot simulate delayed signals. To reduce the amount of accidental background, the detector is shielded by concrete and lead, very dense materials to stop the propagation of gamma rays, as well as by bore-doped polyethylene, a proton rich polymer to slow down through collisions and eventually

stop the progress of neutrons. In terms of the analysis, the aim is to avoid that two non-correlated events taking place by coincidence in the right time interval (ie a cosmic gamma followed by a neutron from the core within the following 45 $\mu$ s) are counted as a neutrino signal. The coincidence time window is reduced to three times the diffusion constant of neutrons. A delayed signal is only taken into account when it takes place between 5 $\mu$ s and 45 $\mu$ s after a prompt signal and no other event occurred in the following 100 $\mu$ s or the precedent 50 $\mu$ s. The amount of accidental noise is evaluated by choosing several windows of 40 $\mu$ s after or after prompt events so that they do not correspond the coincidence window, and then subtracting the energy spectrum obtained from that of coincident events.

Correlated background is made up of events that simulate both a prompt and a delayed signal in a time interval similar to that of the neutrino signal. Fast neutrons (of some 10's of MeV) released by muons, if in the lead shielding for example, or from the reactor core, can collide with several protons in the scintillator, causing their recoil: these protons are energetic enough to cause scintillation, and therefore imitate a prompt signal. The detector's time resolution is not enough to distinguish the different recoiling protons. The neutron diffuses and then thermalises within the liquid, before being captured by a Gd nucleus and therefore providing a delayed signal. The diffusion time being dominant over the thermalisation time, the interval between the pseudo-prompt and delayed signals resembles that in the neutrino signal. If the muon does not cross the scintillator, it does not deposit its characteristic 2MeV/cm in the liquid, which makes its identification impossible that way. For a muon that ends its trajectory in the scintillator by colliding with a C atom, the scenario can be more complex. In order to reject this background, an active muon veto around the detector's shielding stops the acquisition in the 100 $\mu$ s after the detection of each muon. Recoil protons can also be distinguished from positrons as the shape of their electronic signal at PMT's is different. The distribution of events while the reactor is off (fortunately for a substantial amount of time as Osiris is an experimental reactor) can also be studied and deduced from the reactor-on signal in order to attempt to eliminate this background [2].

### **C) Internship work**

The internship lasted 6 weeks at the Saclay CEA centre, at the Orme des Merisiers extension, in the Service de Physique Nucleaire (SPhN), preceded by a week of programming self-teaching. I worked on the Nucifer data analysis. A first part of my contribution to the experiment consisted in optimising the energy, time and Pulse Shape Discrimination (PSD) cuts to be performed on the data to include as much neutrino signal as possible while rejecting as much noise background as possible. I also studied, using Nucifer data, simulation and literature, the  ${}^9\text{Li}$  noise in the detector, an important source of correlated background in neutrino detection.

My main tool was CERN's ROOT software [3], which executes commands in the C++ language. I also took and stored data as well as sent heavy analysis codes onto the IN2P3 processors in Lyon, France. I had the occasion to familiarise with Linux on the laptop I was using during the internship. Other activities include a visit at Osiris and Nucifer with my internship tutor. I presented my work under the shape of short reports on the experiment's web database (ELOG) and gave a small presentation at a Nucifer analysis meeting.

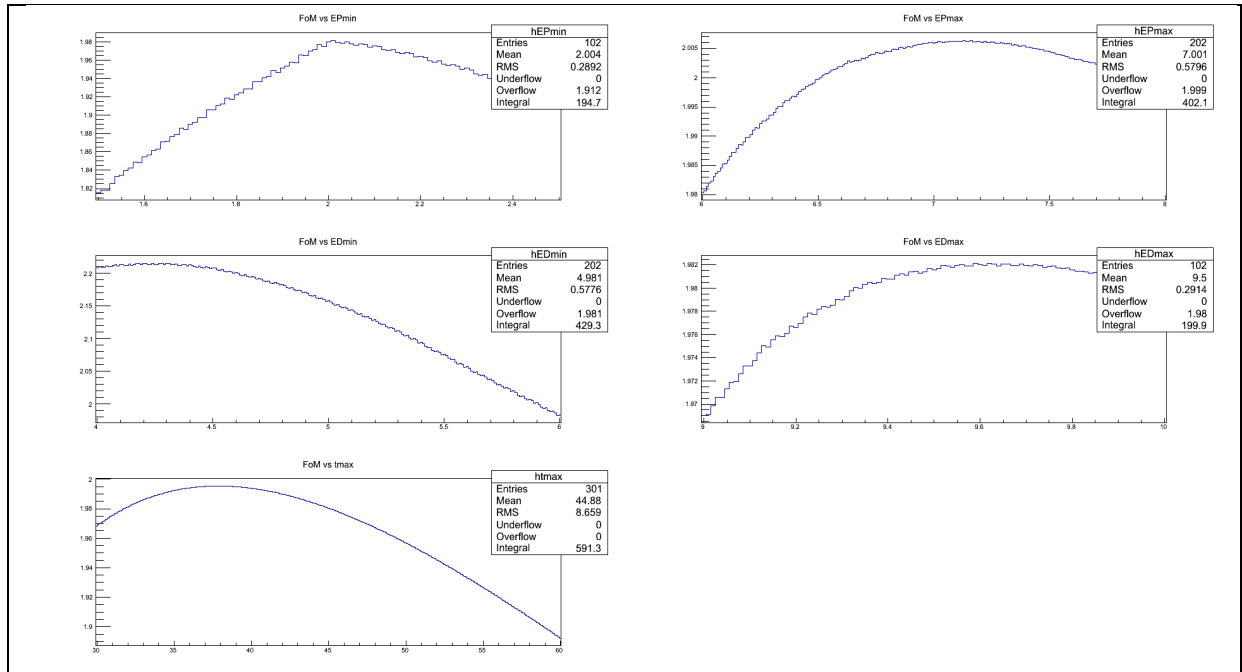
#### **I- Optimisation of energy and time cuts**

In order to isolate neutrino candidates from background noise, the characteristic energies of the prompt (EP) and delayed (ED) signals and the typical time ( $\Delta t$ ) between these is used. The aim is to compute which are the optimal energy and time ranges in which to look for these signals, so as to include as much signal and reject as much noise as possible.

To take cuts maximising signal and limiting both noise and error, a Figure of Merit (FoM) was

obtained: 
$$FoM = \frac{S}{\delta S} = \frac{S}{\sqrt{N_{signal} + (1 + \frac{T_{on}}{T_{off}})N_{off} + \frac{N_{acc}}{w}}}$$

with S the amount of signal, N<sub>signal</sub> the number of detected neutrino candidates when the reactor is on, N<sub>off</sub> the reactor-off number of neutrino candidates, N<sub>acc</sub> the reactor-on number of accidental candidates, T<sub>on</sub> and T<sub>off</sub> the reactor-on and -off times respectively, w the number of time windows opened to look for false delayed candidates for each prompt candidate to measure the accidental noise. As T<sub>on</sub> and T<sub>off</sub> are close for the considered data, the coefficient before N<sub>off</sub> was approximated to 2. The statistical error ( $\delta N = \text{sqrt}(N)$ ) was assumed to be dominant.



From left to right and top to bottom: FoM vs Prompt signal minimal energy EPmin, maximal energy EPmax, Delayed signal minimal energy EDmin, maximal energy EDmax, maximal time between the two signals tmax

In the figure above, the value of the FoM was plotted successively against the energy (in MeV) and time limits for the cuts performed on the data. The numbers of events for the signal are from simulations, whereas correlated noise data was obtained from 20 days of reactor-off measurements and uncorrelated noise from 1 day of reactor-on measurements. For the above plots, the accidental noise was taken to be 4000 events/day.

The nominal cut parameters that have been used so far are EPmin = 2.0 MeV, EPmax = 6.0 MeV for the prompt signal energy, EDmin = 6.0 MeV, EDmax = 10.0 MeV for the delayed signal energy, tmin = 5 μs (the apparatus' response time not allowing to lower this value) and tmax = 45 μs for the time between the two signals. For the plots above, to see which parameters were the most influential on the value of the FoM, the nominal cuts for all other parameters were used while varying one parameter at a time.

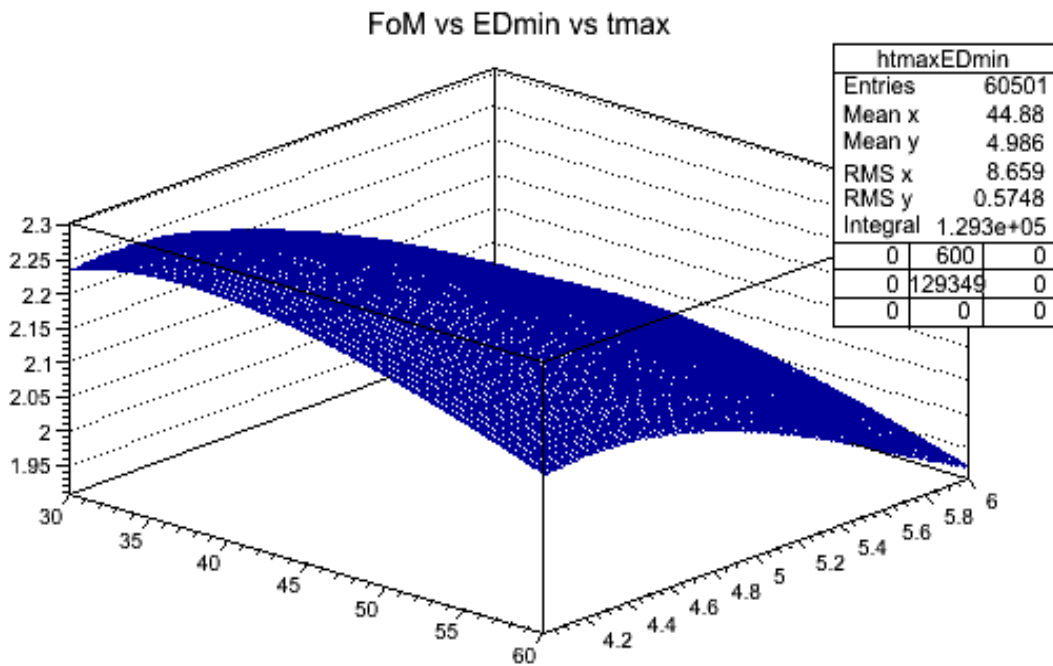
Integrals were taken between the defined limits on the prompt and delayed signals of the reactor-off, and of the reactor-on uncorrelated data as well as of the reactor-on correlated simulation. These integrals were normalised against the reference integrals to obtain the values of  $N_{\text{off}}$ ,  $N_{\text{signal}}$  and  $N_{\text{acc}}$ .

For EPmin, the FoM peaks at 2.01 MeV. The decrease for higher energies (to about 90% of its optimal value at 2.5 MeV) can be explained by the smaller number of prompt candidates in the considered range, and therefore an increase in statistic error. For lower energies, the sharp drop in the number of prompt events and the increase in accidental noise are consistent with the decay observed (also to about 90% of its optimal value at 1.5 MeV). (It is to be noted that for the correlated noise, due to the lack of data below 2 MeV, I extrapolated from the measurements with a 2nd order polynomial.) The influence of EPmax on the FoM is lesser, with variations in the FoM in the order of magnitude of 1% over the 6 to 8 MeV range. The maximal FoM is observed at 7.13 MeV.

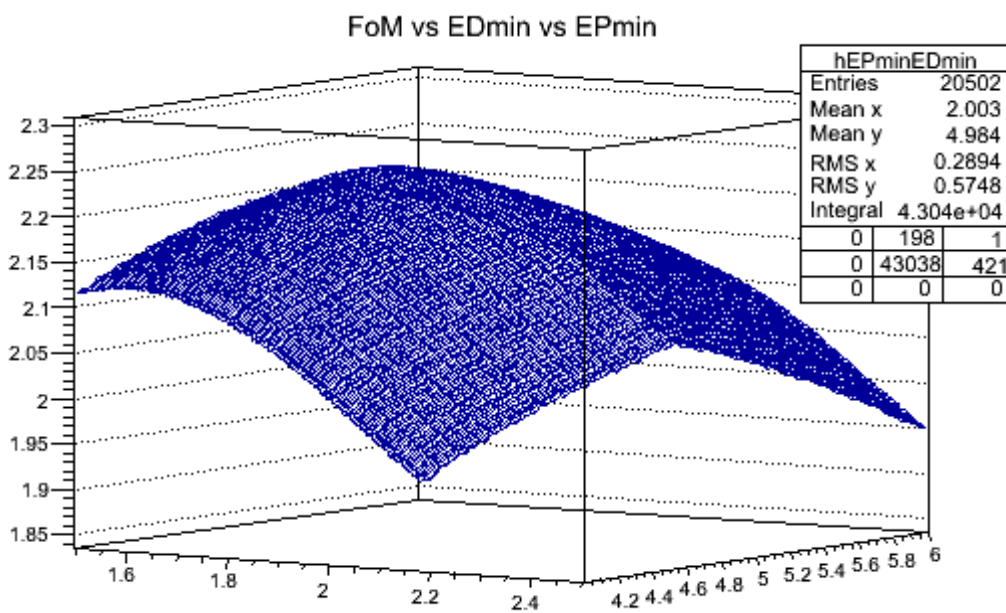


When varying  $E_{dmin}$ , the maximal FoM is at 4.27 MeV, 110% of the nominal value measured at 6 MeV. This may be justified by a roughly constant and high number of delayed candidates on the lower part of the energy range, while there is less accidental noise on this range of higher energies compared to the prompt one. The change in FoM with  $E_{Dmax}$  was around 1%, with a maximum at 9.59 MeV.

The value of  $t_{max}$  (computed using a decreasing exponential correlated signal and a constant accidental noise) was also influential, with variations in the FoM of about 10% as  $t_{max}$  ranged from 30  $\mu s$  to 60  $\mu s$ . The maximal FoM was at  $t_{max} = 37.9 \mu s$ .



The above histogram shows the FoM against  $E_{Pmin}$  and  $E_{Dmin}$ , with other parameters at their optimal values. The FoM was maximal for  $E_{Pmin} = 2.01$  MeV and  $E_{Dmin} = 4.18$  MeV.



Above was plotted the FoM against EDmin and tmax, with other parameters at their optimal values. This time EDmin = 4.18 MeV and tmax = 37.3  $\mu$ s.

I also obtained from computation, varying at the same time the 3 most influential parameters, that the maximum value of the FoM = 2.26 day<sup>-1/2</sup>, reached when EPmin = 2.0 MeV, EDmin = 4.2 MeV, tmax = 40  $\mu$ s which is consistent with the values in the above paragraphs.

From this study the cuts that would seem optimal to me so far are:

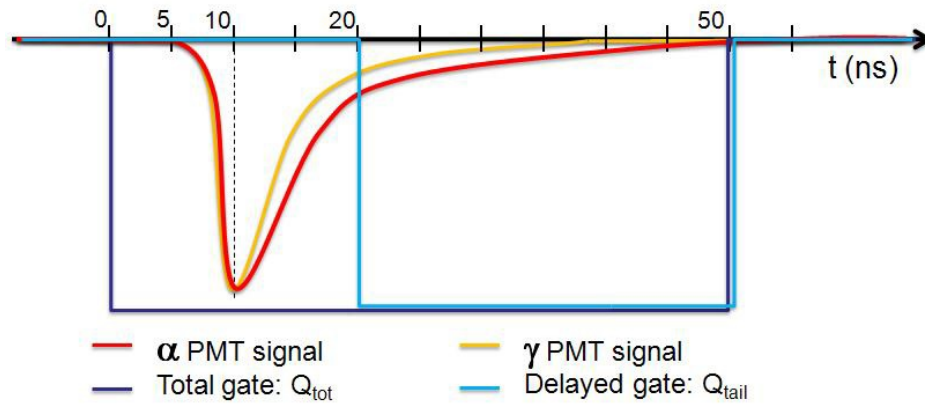
	minimum	maximum
Prompt signal energy (MeV)	2.01	7.13
Delayed signal energy (MeV)	4.18	9.59
Time between the signals ( $\mu$ s)	5.0	40

Noise(/day)	EPmin(MeV)	EDmin(MeV)	tmax( $\mu$ s)
8000	2	4.3	40
7000	2	4.3	40
4000 (present)	2	4.2	40
2000	2	4.1	40
133 (after Pb shielding)	2	4	57

The table above lists the optimal cuts for several amounts of accidental noise per day, ie the cuts that maximise the FoM. Overall, the dependence of the optimal cuts on the amount of noise is very slight. Changes are most notable for the least amount of noise 133 events/day. For ED and tmax, the very important drop in noise allows us to study larger ranges to collect more signal while not collecting as much noise as before.

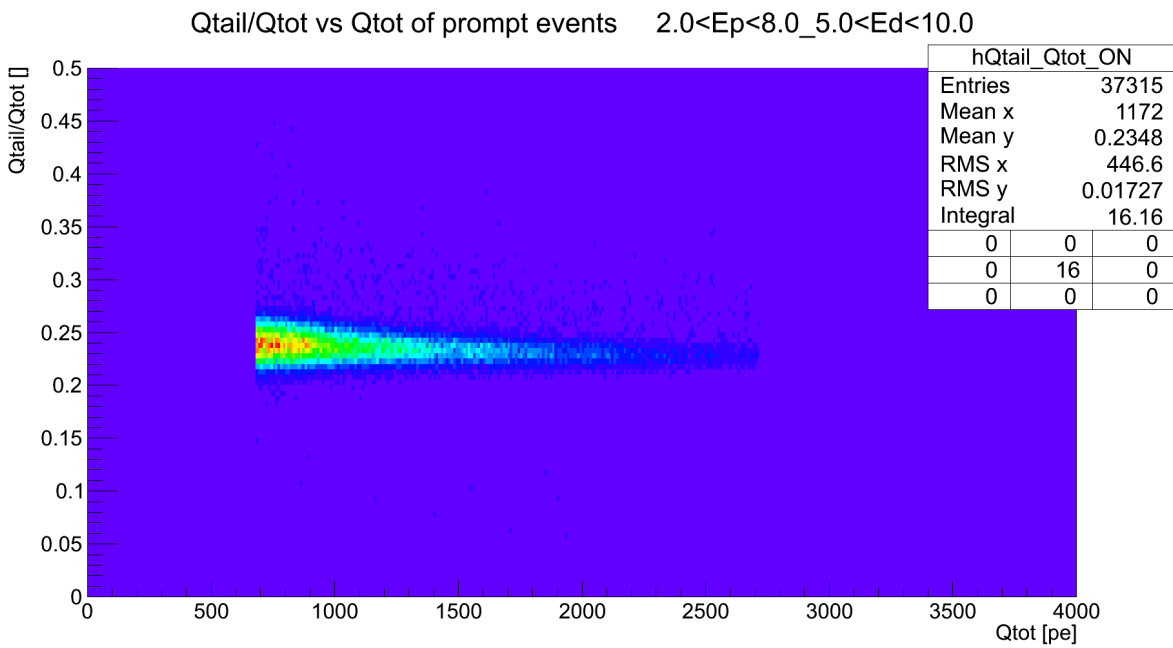
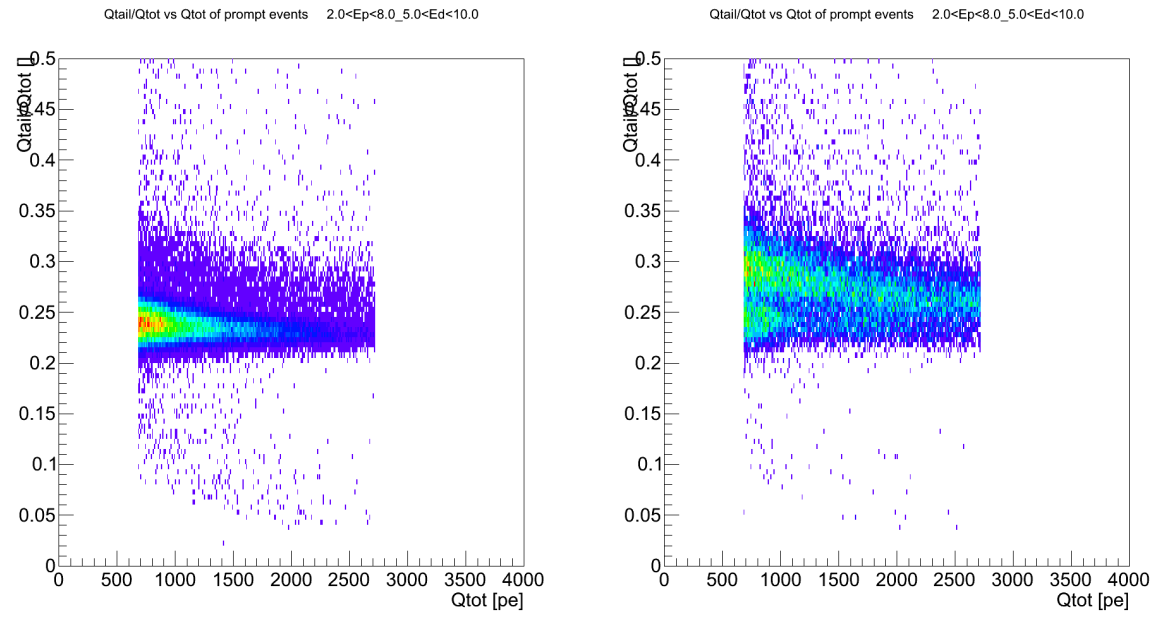
## II- Optimisation of the PSD cut

Pulse Shape Discrimination (PSD) is a recurrent technique in signal detection physics. In our case, it allows us to distinguish a positron/electron/gamma signal from a recoil proton signal, in order to reject the fast neutron correlated background. For an equivalent kinetic energy, a recoil proton or neutron will be slower than a positron, electron or gamma. Therefore, the number of ions formed per unit path length, or ionisation density, is more important for the recoil proton. In first order terms, the greater ionisation density leads to a larger part of the energy dissipated as heat rather than scintillation (“quenching” effect). In second order terms, it favours long-life excited states to short-life ones. Thus the shape of the pulse signal for recoil protons and neutrons will tend to be more spread out for neutrons and protons than for electrons, positrons and gamma rays. For the same Q<sub>tot</sub> (total energy released) the latter part or tail of the signal Q<sub>tail</sub> will include a larger proportion of the signal [2].



Plotting the number of detected events is plotted vs  $Q_{tail}/Q_{tot}$  vs  $Q_{tot}$ , we can observe higher band presumably made up of recoil proton events and a lower one made up of positron, electron and gamma events. It is also expected that the accidental signal will be dominated by gamma rays, the reactor-off correlated one by recoil protons from fast neutrons and the reactor-on correlated one by positrons from the neutrino prompt signal. In this part, I have considered the way to discriminate the positron signal from the recoil proton background from the event plots vs  $Q_{tail}/Q_{tot}$  vs  $Q_{tot}$ .

**a) Shape of the plots vs  $Q_{tail}/Q_{tot}$  vs  $Q_{tot}$  and of the PSD cut**



Reactor-off data was obtained from March, May and June runs. Reactor-on data came from the April and May runs. The histograms of the number of event pairs against  $Q_{tail}/Q_{tot}$  and  $Q_{tot}$  were cumulated for both cases (first plot above, OFF on the left and ON on the right). To eliminate the cosmic correlated noise, the off-distribution was subtracted off the on- one, with both being normalised to give the number of events per day (second plot above).

The above plot shows the sum of the on- and off- distributions for a better visualisation of the two regions: the upper one due to proton motion (ie noise) and the lower one due to electrons, positrons and gamma rays (ie signal).

In the following figure, the nominal cut is at  $Q_{tail}/Q_{tot} = 0.26$  (in white). It can be guessed from the graph that to get a cut that includes more signal and less noise, one may try an oblique line, or even two oblique lines (ie in black).

The goal is to look for a new cut that includes as much neutrino signal as possible and as little background as possible, ie maximise the quantity  $S/\delta S$ , where  $S$  is the neutrino signal and  $\delta S$  the error in this signal, with all quantities normalised per day:

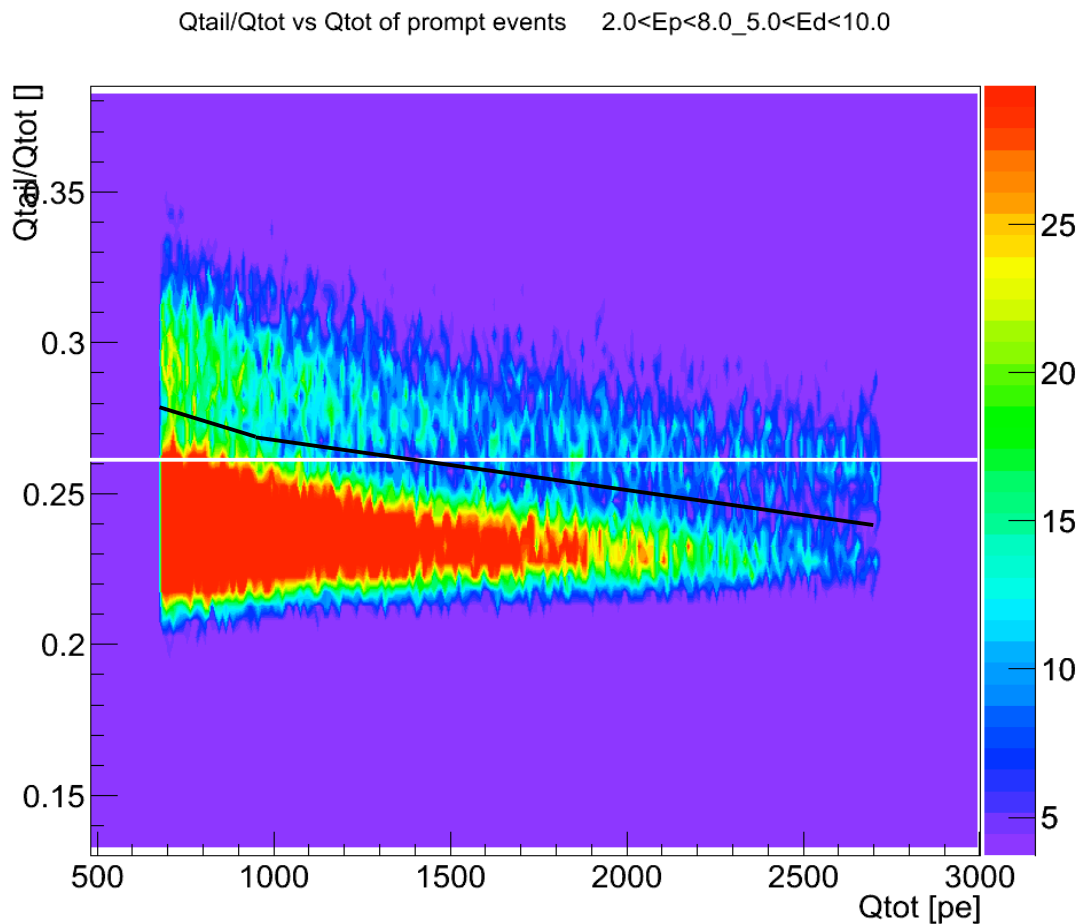
$$S = N_{on} - N_{off} - N_{acc}$$

Therefore if we suppose the statistical error ( $\delta N = \sqrt{N}$ ) is dominant, after a short derivation the error in  $S$  is given by:

$$\delta S = \sqrt{N_{on} + N_{off} + N_{acc}}$$

This  $S/\delta S$  figure can be maximised by varying the coordinates of the points on the two straight lines.

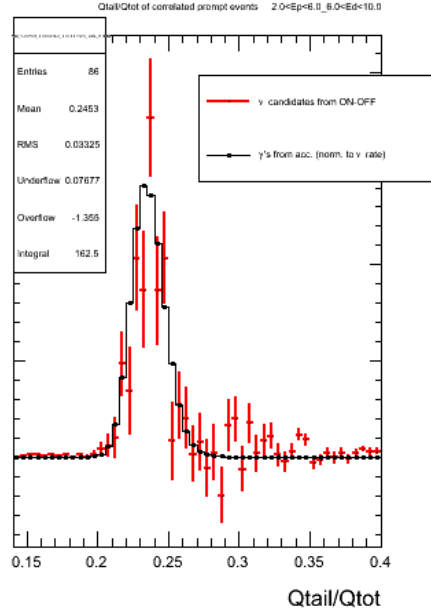
In order to perform this study, we would need the plot of  $N_{acc}$  vs  $Q_{tail}/Q_{tot}$  vs  $Q_{tot}$ , which can be obtained from re-running the data analysis codes.



### b) Analysis and optimisation with accidental reactor-on events

This analysis was performed over about 20 days reactor-on and 63 days reactor-off. The statistical error in the correlated data itself being too great to determine with accuracy the distribution of

neutrino candidates (reactor-on signal - reactor-off signal - accidental noise) vs  $Q_{tail}/Q_{tot}$  vs  $Q_{tot}$ , reactor-on accidental noise was used to optimise the PSD cut. Indeed, accidental gamma rays show the same signal shape against  $Q_{tail}/Q_{tot}$  (see figure below) and provide a large amount of data available. The noise was considered to be dominated by correlated reactor-off signal, ie accidental reactor-off background subtracted from total number of reactor-off correlated candidates [4].

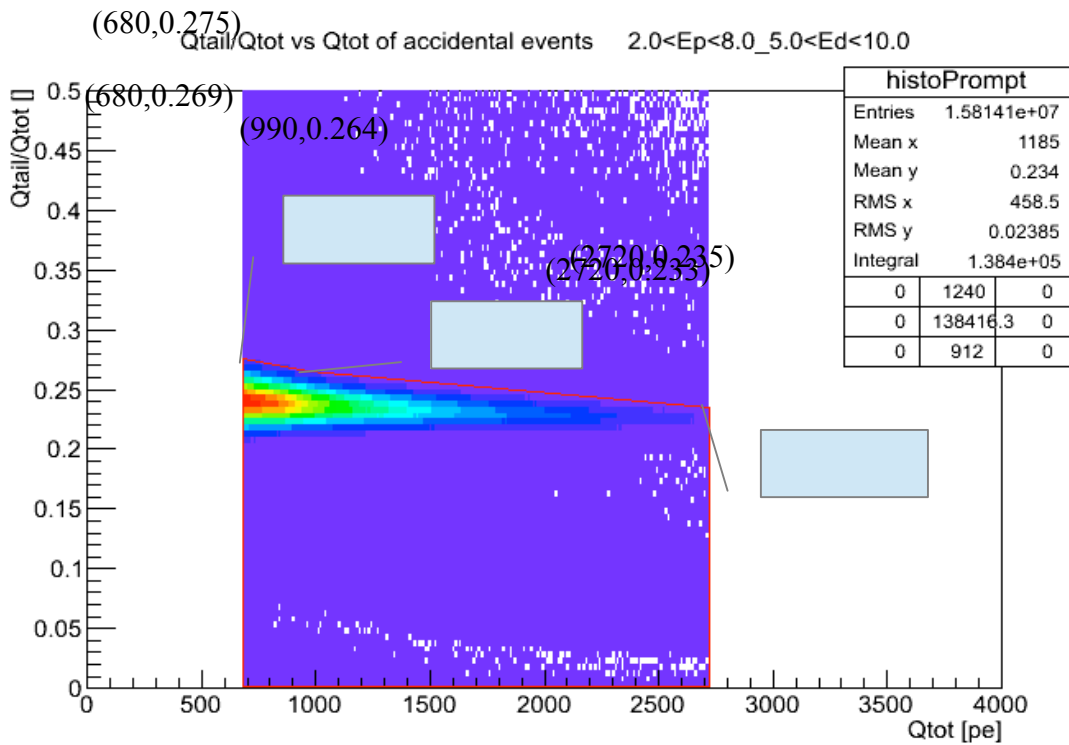


With this assumption, the uncertainty in the signal becomes:

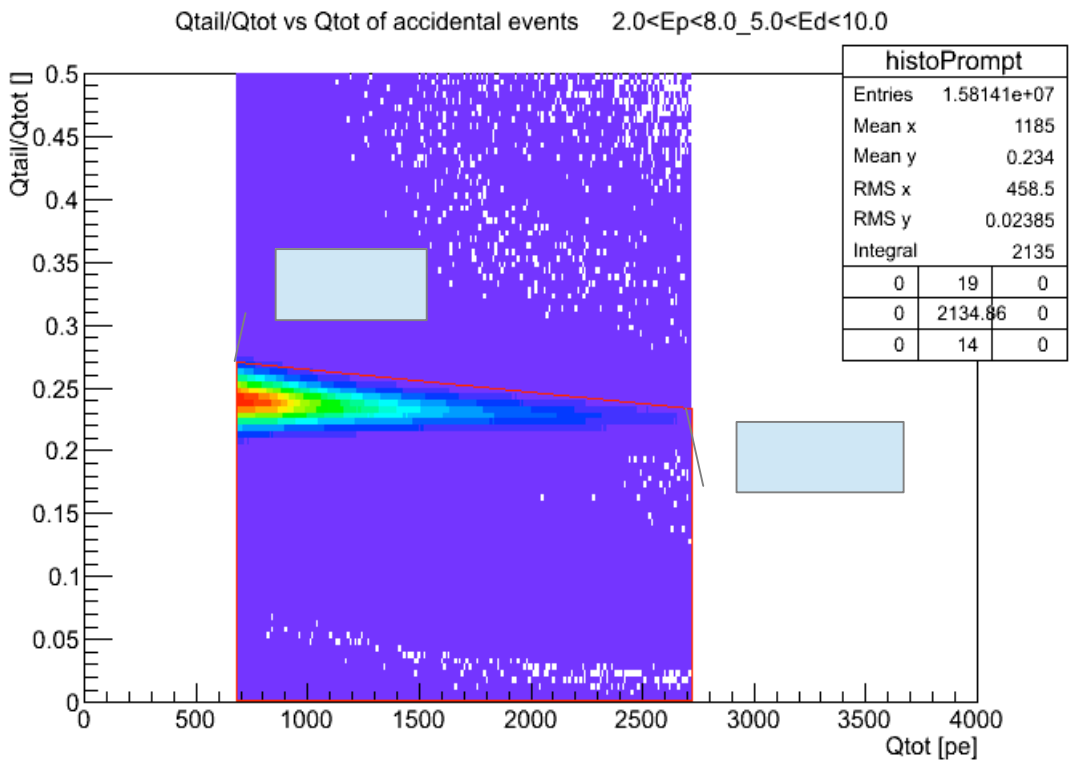
$$\delta S = \sqrt{N_{acc} \left( 1 + \frac{1}{w} + \frac{1}{\left(\frac{f_{acc}}{\nu}\right)^2} \right) + \left( 1 + \frac{norm_{ON}}{norm_{OFF}} \right) N_{OFF}}$$

still considering the statistical error as dominant,  $N_{acc}$  the number of accidental candidates and  $N_{off}$  the number of reactor-off ones within the region below the cut, with  $f_{acc}/\nu$  the ratio of accidentals to neutrino candidates,  $w$  the number of windows opened to evaluate the amount of uncorrelated noise,  $norm_{ON}$  and  $norm_{OFF}$  the normalisation factors to scale the histogram down to the same integral in the recoil protons region.

I wrote a code using the double-line cut suggested above, allowing their slopes to be varied and optimised. I obtained the optimal cut shown in the following figure: 2% of the neutrino signal (ie the accidental reactor-on signal) were rejected, while 24% of the reactor-off correlated signal were included.

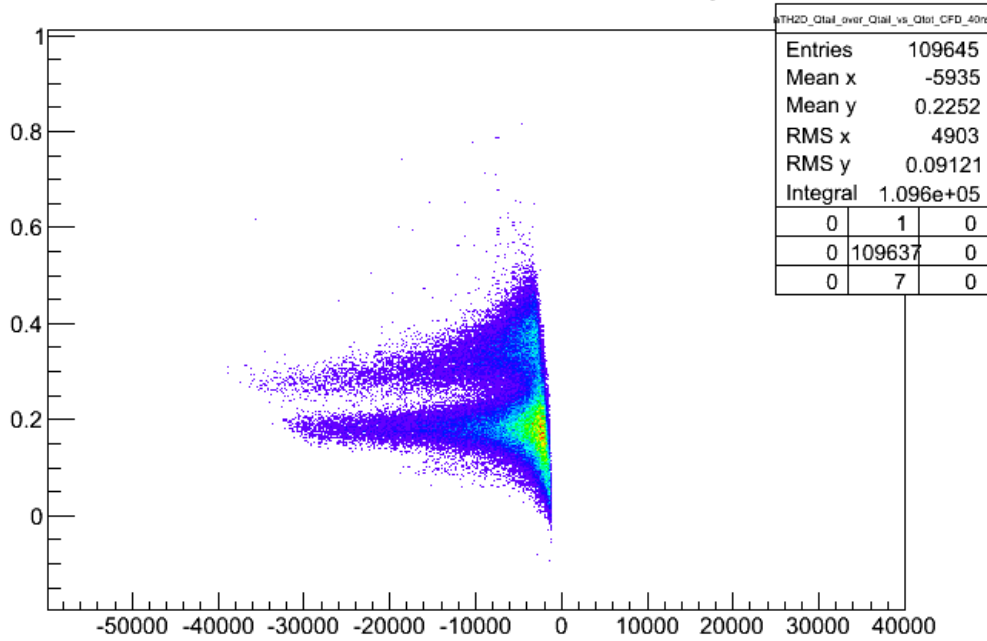


With a single line cut, an almost as good optimisation is obtained, with 3% of signal rejected and 22% of noise included, as shown below.



The next step is to program this PSD cut into the analysis algorithm together with the optimised energy and delta t cuts and re-analyse the data from the past few months.

Qtail/Qtot vs Qtot, time with CFD, delay 40 ns



Interestingly, it can be observed that the positron/electron signal plotted vs Qtail/Qtot vs Qtot is about constant with Qtot, whereas the proton signal shows in the above figure a decreasing trend in Qtail/Qtot as the Qtot energy increases. This also appears for a different liquid and experimental setting, here 20% PXE, 70% LAB et 10% bisisopropylnaphtalene in a test cell.

### c) Summary of results with all new cuts

The analysis codes were re-run over 31 days reactor-on and 45 days reactor-off. Results with the nominal cuts and with the new ones are summarised in the following table.

Analysed data		With previous nominal cuts	With new cuts
Reactor-ON (events/day)	Correlated	262	443±16
	Accidental	4000	8909
Reactor-OFF (evts/day)	Correlated	124	216±2.5
	Accidental	30	78
<b>Neutrino Candidates (Reactor-ON – Reactor-OFF)</b>		<b>138</b>	<b>227±16</b>
<b>Increase in the FoM</b>		<b>-</b>	<b>13%</b>

A larger number of all detected events was expected due to the opening of the energy ranges considered. The increase in the FoM is consistent with expectation, while being limited by the large amount of accidentals included in the lower prompt energies by the PSD cut. The significant increase in the number of neutrinos may be very significant for more accurate and precise physical data, especially when an extra lead shielding is added to substantially lower the amount of accidentals. The optimisation work can be considered to have yielded conclusive results.



### III- Analysis of the ${}^9\text{Li}$ background

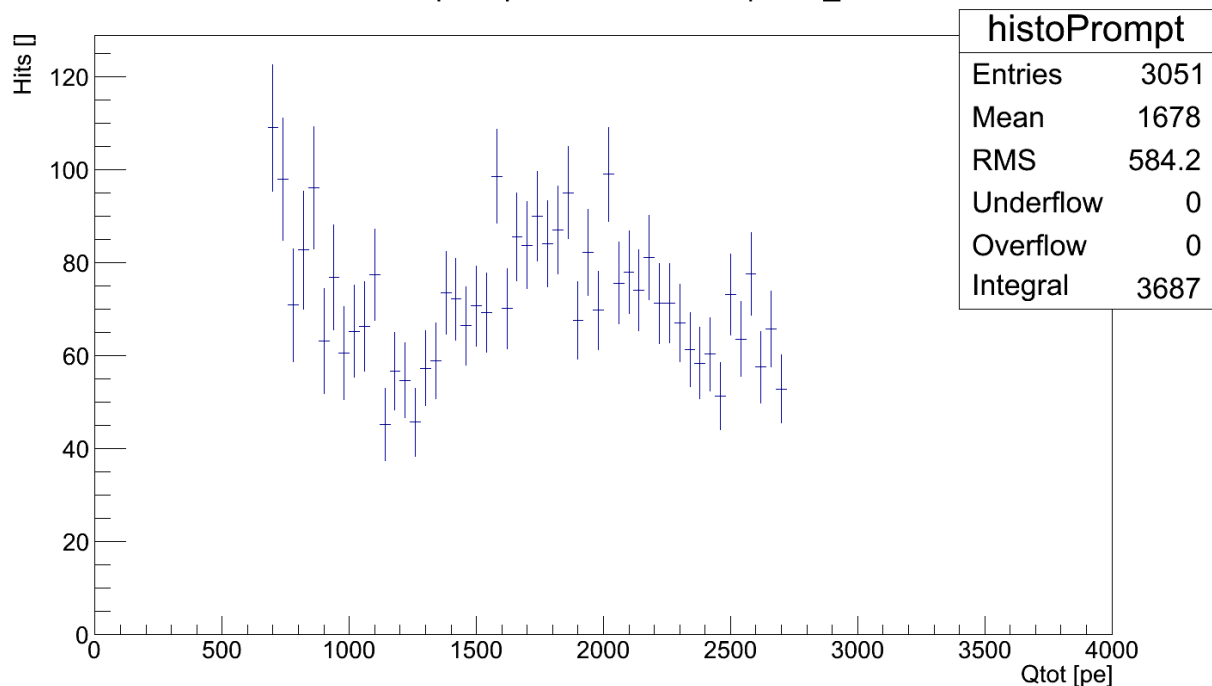
${}^9\text{Li}$  is an important concern in neutrino detection as a source of correlated background. Stopping cosmic muons in the scintillating liquid can collide with a C nucleus, depositing an energy of the order of magnitude of several GeV. This collision fragments the nucleus into multiple particles, of which can be a  ${}^9\text{Li}$  nucleus.  ${}^9\text{Li}$  having an excess of neutrons for its number of protons, it decays into  $\beta$ -n radioactivity, releasing an electron and a neutron.

The electron annihilation with a positron, from a neutrino and proton inverse  $\beta$  reaction for example, provides a simulated prompt signal, while the neutron mimicks the delayed signal. As the half-life of  ${}^9\text{Li}$  is relatively long (0.178 s) it is difficult to exclude this background with a muon veto [4].

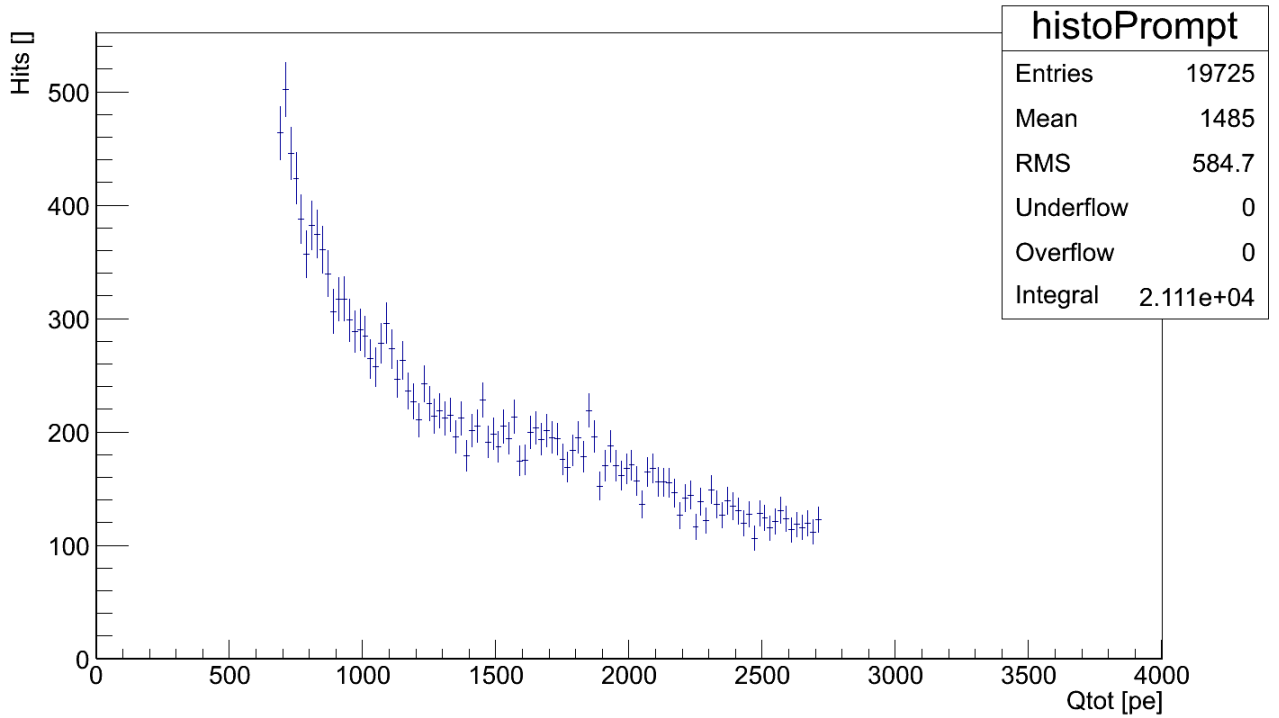
It is therefore important to study the amount, energy distribution and fluctuation in this background to be able to reject it in Nucifer or to understand its variation with depth, detector dimensions or scintillating liquid volume and composition in order to predict its spectrum in other experiments. In particular, the results from the Double CHOOZ (DC) experiment (far-field two-detector setup studying two commercial reactors) show the eventuality of a linear trend relating the number of  ${}^9\text{Li}$  to a number of detector characteristics. It would thus be interesting to compare the Nucifer results (at a much shallower depth and for a much smaller detector volume) to these. For this study, I estimated the number of  ${}^9\text{Li}$  events from extrapolation and re-scaling of DC data and seeked to compare it with the results obtained from data analysis.

#### a) How the ${}^9\text{Li}$ question first arose, or ‘The Bump’

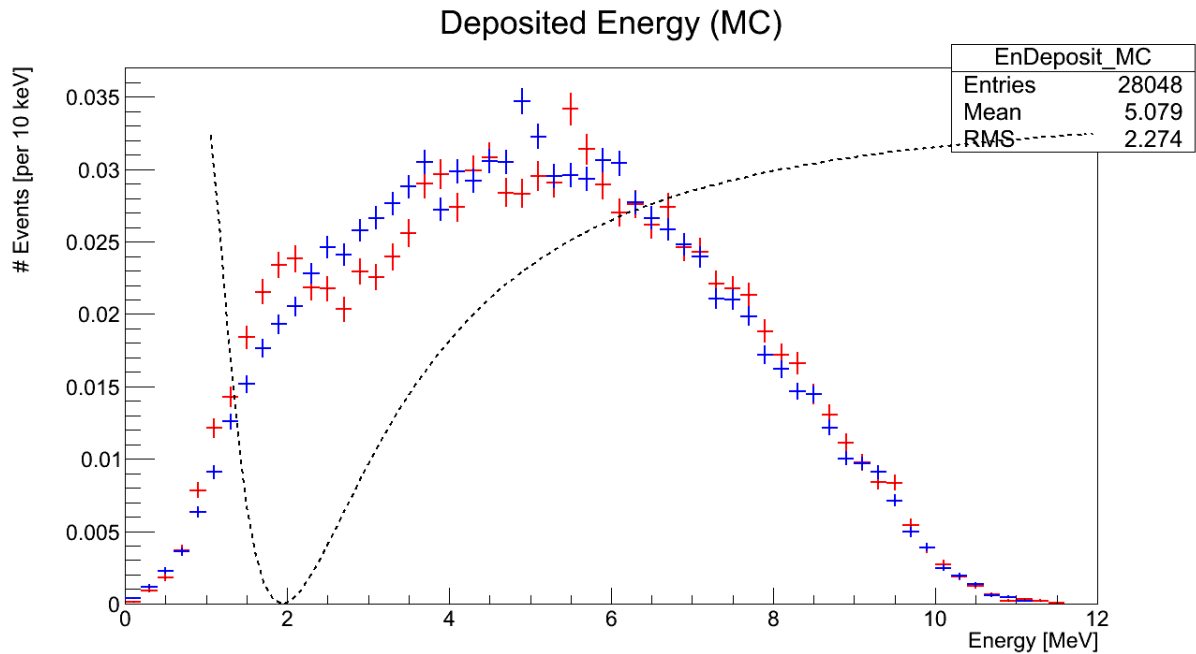
Qtot of correlated prompt events  $2.0 < E_p < 8.0$   $5.0 < E_d < 10.0$



Qtot of correlated prompt events 2.0<Ep<8.0\_5.0<Ed<10.0

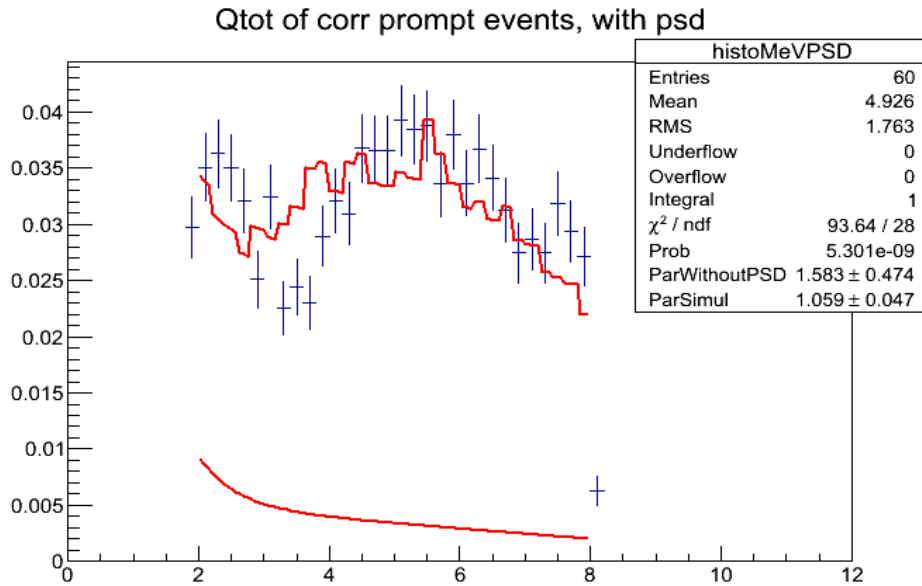


In the two figures above, the reactor-off Prompt data with PSD, from about 20 days of runs from March, May and June, shows a distinctive maximum around  $Q_{tot} = 2040$  pe, i.e. 6 MeV (first plot). It is much less visible in the same data without PSD (second plot). The hypothesis may be made that this maximum in the PSD function could be due to  ${}^9\text{Li}$ . The energy at the maximal number of events could be compatible, looking at the simulation of the  ${}^9\text{Li}$  signal for DC shown below.

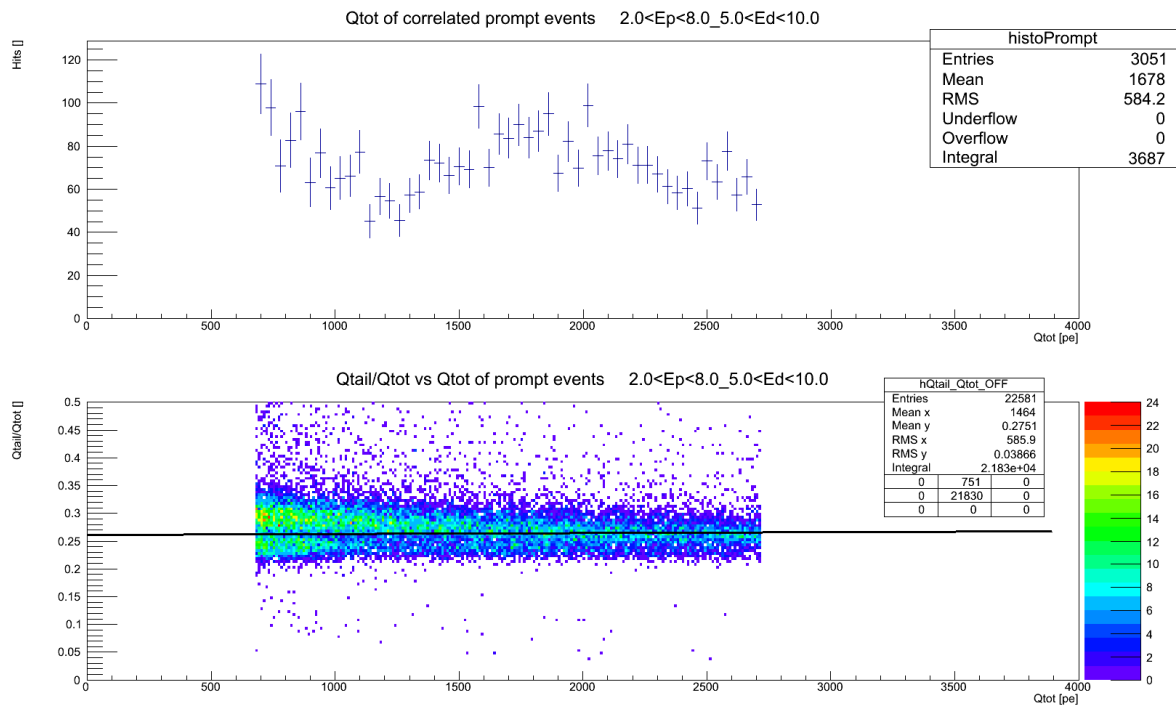


The electron released in the  $\beta$ - disintegration of the  ${}^9\text{Li}$  nucleus would pass the PSD cut, which is consistent with the bump being more observable in the histogram with PSD. In other terms, the  ${}^9\text{Li}$  electron signal would get lost among the other signals.

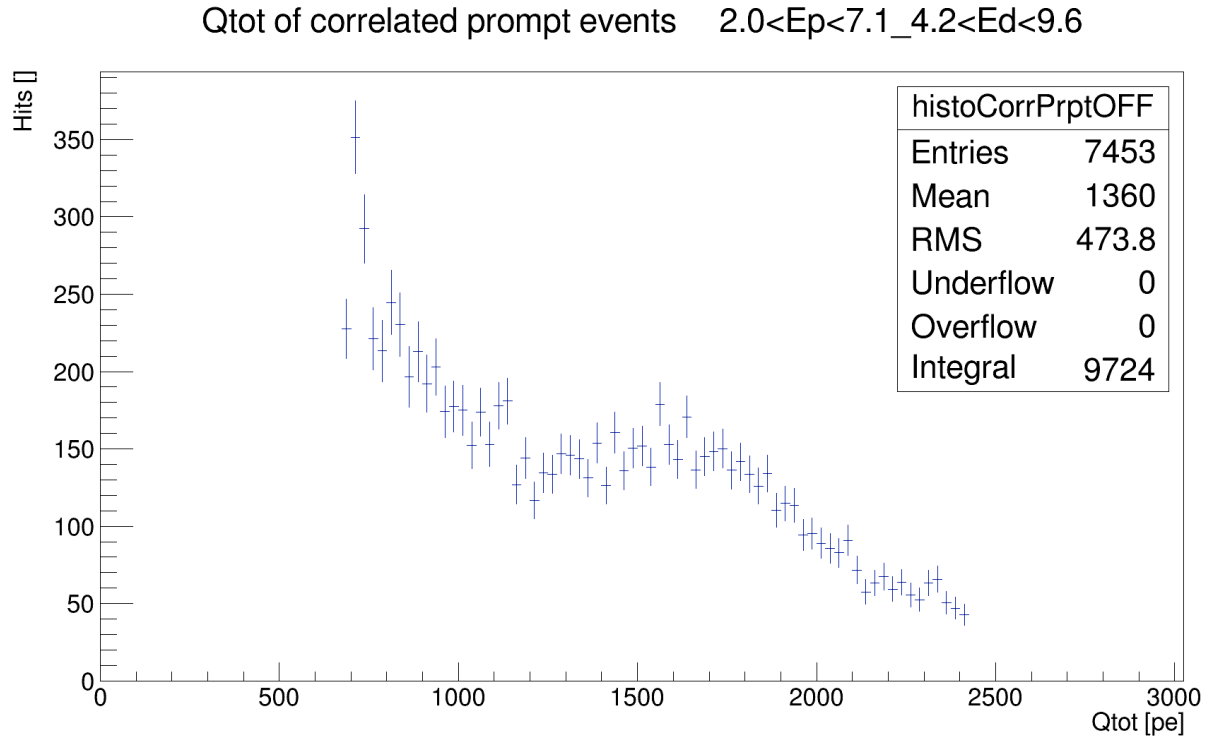
The idea was to suppose that all these other signals would pass the PSD cut in smaller and equal proportions, such that the signal with PSD can be described as the weighted sum of the signal without PSD and the  ${}^9\text{Li}$  simulation. Then, I attempted to fit the PSD histogram with such a sum, shown in the following plot.



The data points are in blue and the fit in red in the upper part. The red line at the bottom of the figure is the contribution of the data without PSD to the fitted data. It was estimated from this plot's integral that the number of  ${}^9\text{Li}$  events per day would be around 134 which is extremely important (only 1  ${}^9\text{Li}$  event per day is measured in DC). This striking number was the first trigger to a study of  ${}^9\text{Li}$  background in Nucifer.



I figured out later on that the observed ‘bump’ may not be related to  ${}^9\text{Li}$  noise, as shown in the above figure. Indeed the number of correlated events increases in the energy region in which the recoil proton band in the  $Q_{\text{tail}}/Q_{\text{tot}}$  vs  $Q_{\text{tot}}$  plot passes below the nominal cut, shown in black. Therefore, it is now agreed that, rather than  ${}^9\text{Li}$ , the main contributor to this bump is a misplaced PSD cut which would result in recoil protons simulating prompt events for energies high enough (as  $Q_{\text{tail}}/Q_{\text{tot}}$  tends to decrease, see plot above). If this is true, a consequence would be that the bump is less apparent in the results from the analysis with the new, sloping PSD cut.



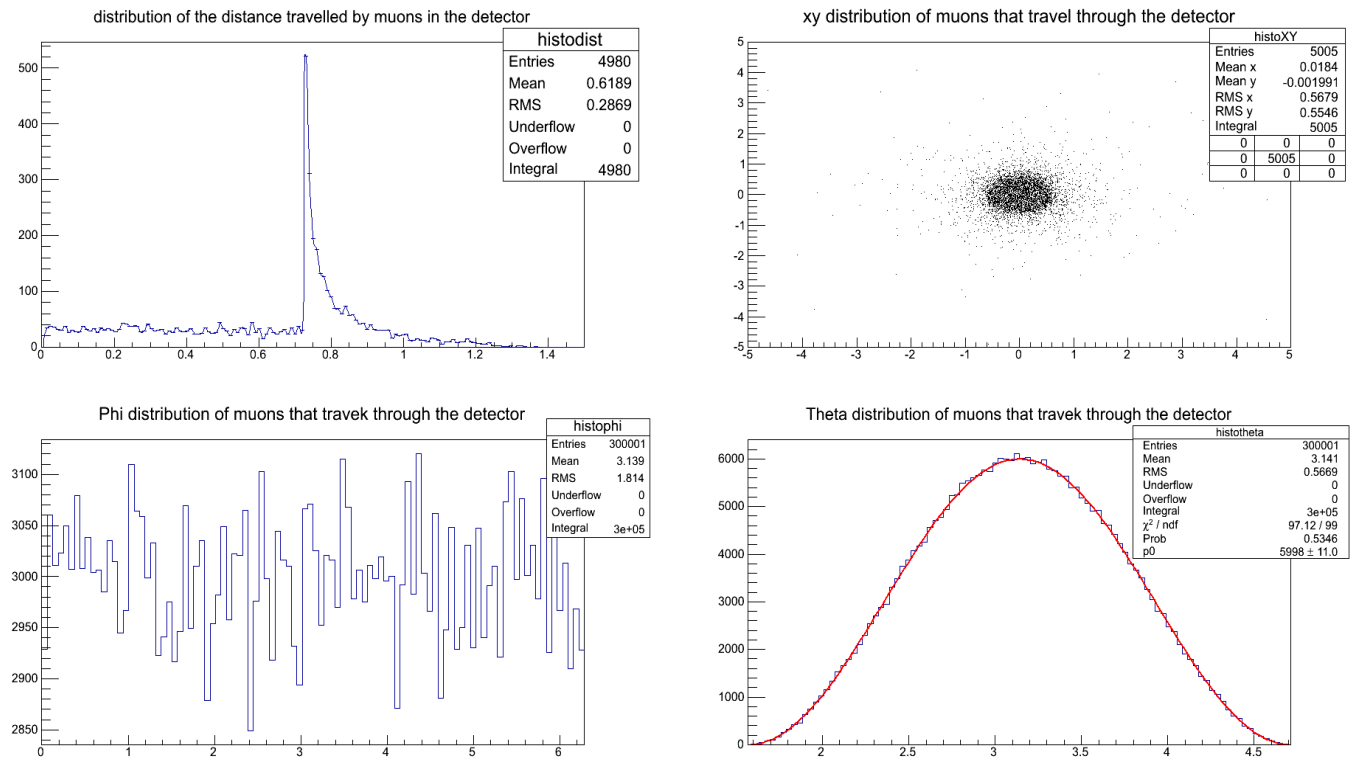
After re-analysing with the new cuts, it can be observed the ‘bump’ is much less prominent than before (see above), showing the same shape as in the plot without PSD. This tends to corroborate the idea that the initial shape may be due mostly to recoil protons.

### b) Estimation of the number of ${}^9\text{Li}$ events in Nucifer from extrapolation of DC data

The estimation is performed from extrapolating the DC results [5] to Nucifer. This requires rescaling the number of carbon nuclei, the muon flux and the mean muon energy.

With the present Nucifer scintillating liquid (50 wt% PXE, 50 wt% dodecane), there are  $3.18 \cdot 10^{28}$  C nuclei in the scintillator. To derive the muon flux, one has to divide the total measured muon rate by the effective detector area, of which a good approximation is the detector volume divided by the average path length a muon travels within the scintillating liquid. I estimated this mean distance with a simple simulation, approximating the number of cosmic muons from all directions around Nucifer to be equal (in reality the muons from the reactor side would be less as many would be blocked by the pool water). The detector is considered as a cylinder, where the origin of the cartesian axes is the centre of the bottom circle and the z axis is the vertical cylinder axis. Muons are launched from a horizontal  $10\text{m} \cdot 10\text{m}$  surface hovering  $0.75\text{m}$  above the detector bottom with an angle  $\varphi$  with the x-axis and an angle  $\theta$  with the z-axis. The start position of the muon and the  $\varphi$  angle are drawn at random from a uniform distribution, while  $\theta$  follows a  $\cos^2\theta$  probability distribution. The distance

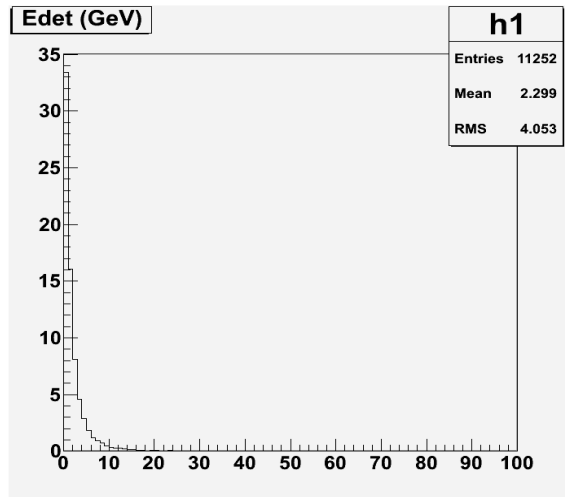
between the two intersections (if any) of the straight line generated and the cylinder is computed and plotted into a histogram as shown below.



For a verification, the plots below show the distribution of the distance travelled in the liquid and the x,y,  $\theta$  and  $\phi$  distributions for 300 000 muons. As expected, the distribution of muons does not show any dependence on  $\phi$  (should be flat for more events), and the distribution over  $\theta$  has a maximum at  $\pi$  and roughly the shape of  $\cos^2(\theta)$ , while the x-y distribution shows that the greatest density of muons is attained directly above the detector. The distance distribution also reaches a clear peak at 0.73m which is the height of the liquid in the detector. Simulating 10624990 muons, of which 177142 crossed the scintillator, the mean travelled distance through the liquid was 0.6182 m.

The muon rate obtained from the data is 115.7492  $\mu/s$ , measured from the number of events saturating all PMT's over one day. This results in a muon flux of 2.9e+2  $\mu/s/m^2$ .

A MUSIC/MUSUN simulation previously run for Nucifer gave a mean muon energy of 2.3 GeV. The energy spectrum is shown below.



In order to estimate the number of Li events that can be measured, it is also important to consider the duration of the muon veto in Nucifer and DC experiments. It is of only 100  $\mu$ s for Nucifer, against, in DC, 500ms when the muon energy is greater than 600 MeV and 1ms otherwise. Considering that half of  ${}^9\text{Li}$  nuclei are formed below 600 MeV and that the half-life of  ${}^9\text{Li}$  is 178.3 ms, the number of expected  ${}^9\text{Li}$  events to measure in Nucifer should be scaled upwards by a factor 4.00.

Then, by extrapolating, I found 1.09  $\beta$ -n background events/day from DCI results and 0.68 events/day from DCII results [5].

All important results for the re-scaling are summarised in the following table:

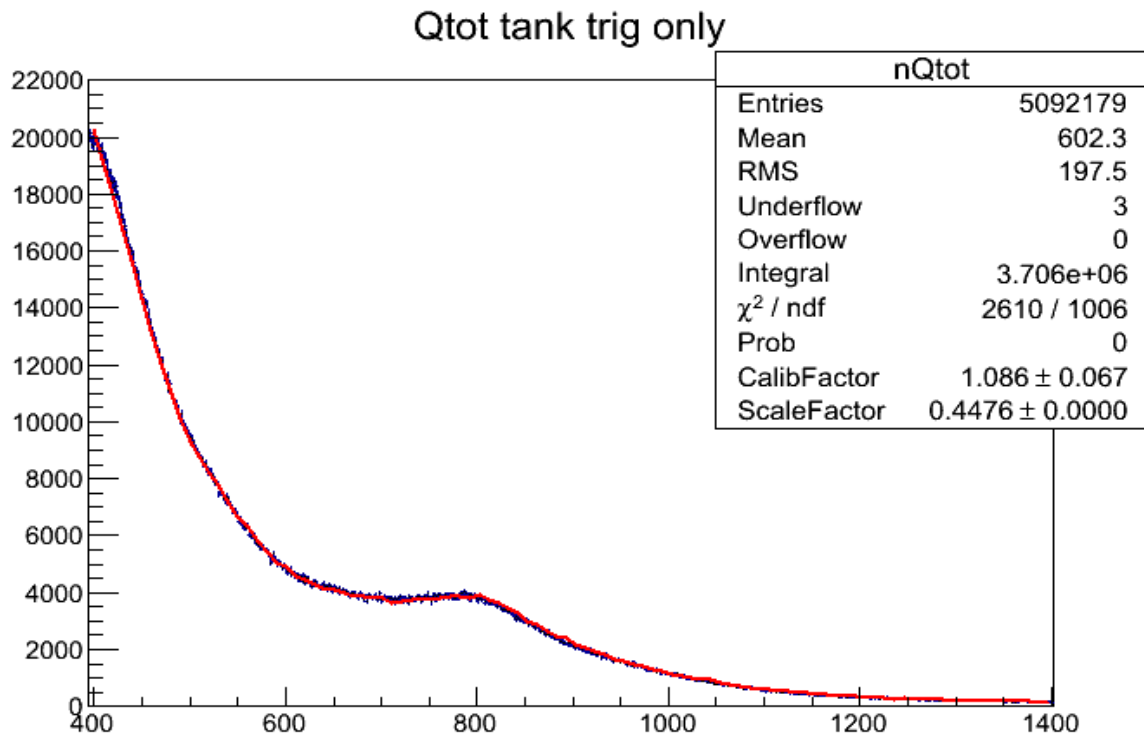
Physical Quantity	Value	Comments
Number of C nuclei	$3.18 \cdot 10^{28}$ C	-
Mean distance travelled by muons	0.6182 m	Simulation, within the scintillating liquid (cylinder)
Muon rate	115.7492 $\mu$ /s-1	Events saturating all PMT's in one day
Muon flux	$2.9 \cdot 10^2$ $\mu$ /s/m <sup>2</sup>	Effective detection surface estimated using scintillator volume/mean distance travelled through liquid
Mean muon energy	2.3 GeV	MUSIC/MUSUN simulation
Re-scaling factor due to veto lifetime	4.00	Supposing $\frac{1}{2}$ of ${}^9\text{Li}$ events happen with muons less energetic than 600MeV
→ Estimate from extrapolation	(From DCI) <b>1.36 evts/day</b> (From DCII) <b>2.72 evts/day</b>	From plot on article [5]

The estimation is to be compared with an analysis of the data acquired while the gain of one PMT was lowered, so that only stopping muons saturate all PMT's.  ${}^9\text{Li}$  events are going to be identified by looking for correlated pairs 2 s after stopping muon events.

c) Estimate through data acquisition and analysis

To identify very energetic stopping muons releasing several GeV of energy, that can give rise to  ${}^9\text{Li}$  events, the voltage delivered to PMT Ch8 was decreased from 1085 V to 650 V so that it is saturated only for the most energetic stopping muons. The prompt and delayed candidates, around some MeV of energy, cannot be measured by this PMT, therefore it does not perturb the standard data acquisition.

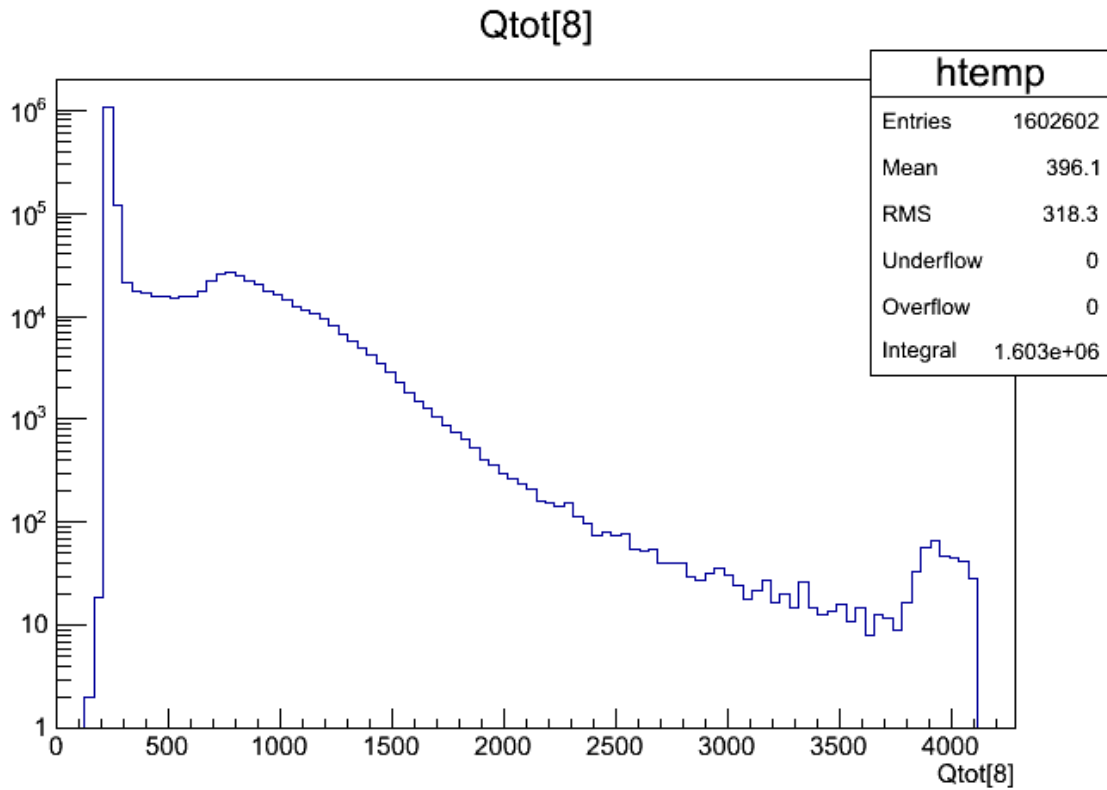
The new calibration factor, obtained by horizontal re-scaling the  $Q_{\text{tot}}$  plot, is 313 pe/MeV. The histogram below shows the new  $Q_{\text{tot}}$  spectrum (in blue) fitted (in red) with the spectrum from a reactor-off run taken in March. The two plots seem to superpose very well.



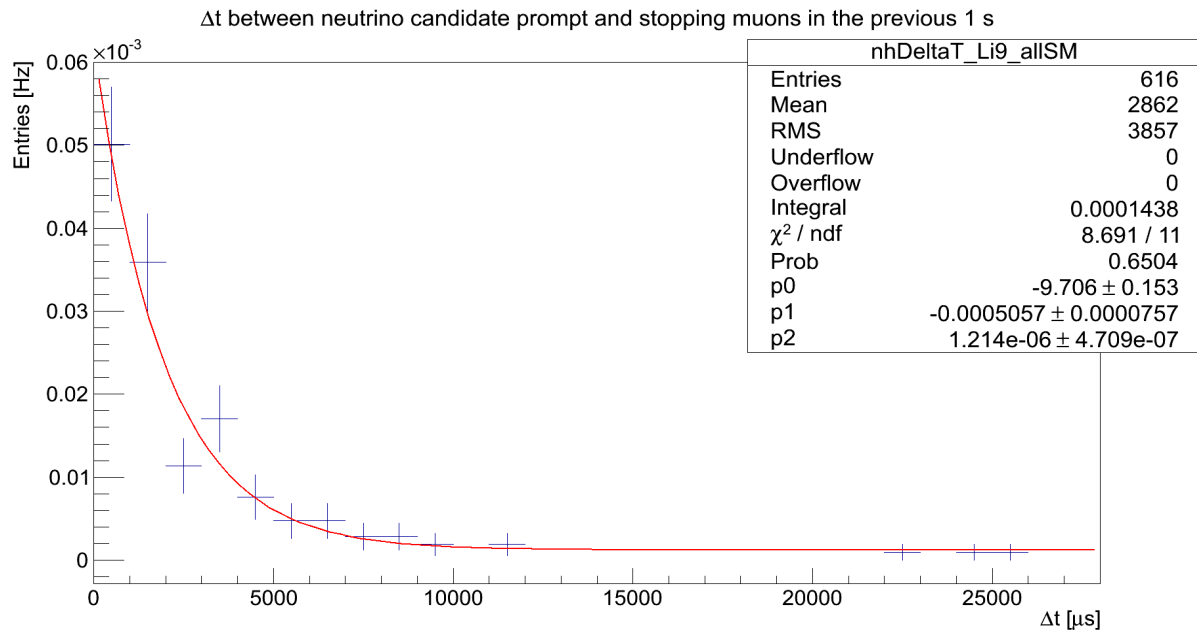
I wrote a code to perform the following analysis, consisting in several steps:

- identifying stopping muons as those exceeding a given minimal energy at the PMT CH8
- identifying neutrino candidates, as usual, with the new energy,  $\Delta t$  and PSD cuts
- for each neutrino candidate, searching for all stopping muons in the 25s preceding the prompt signal and saving their time
- for each of these, plot the time interval between the stopping muon event and the considered prompt event in a histogram vs  $\Delta t$ .

The range of minimal muon energies can be evaluated from the energy spectrum at PMT CH8 in the figure below.

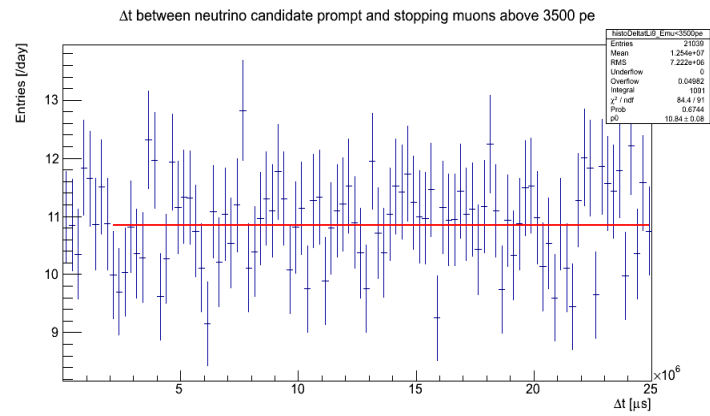
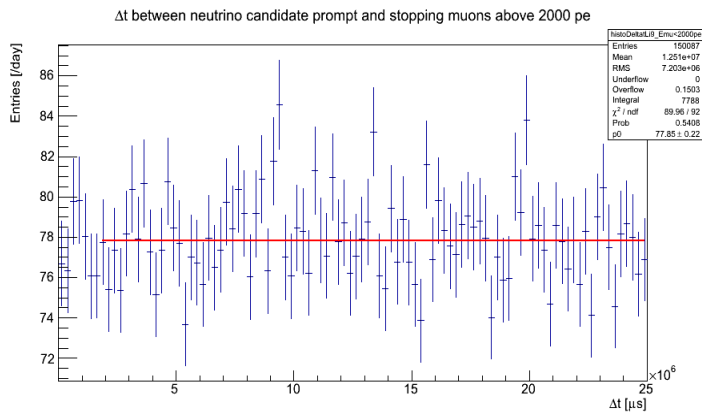
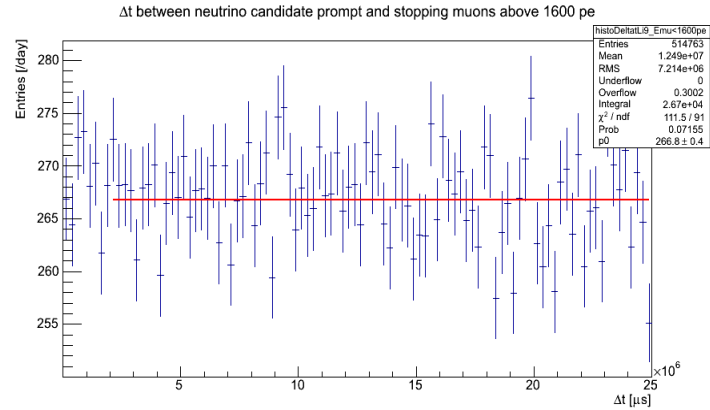
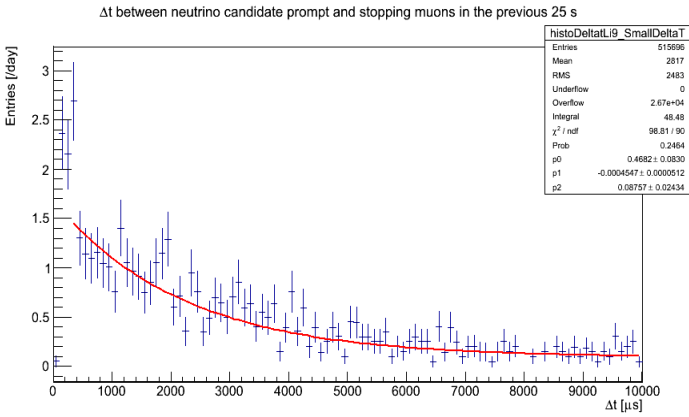


The proposed analysis was run a first time, only for muons saturating the PMT, i.e. in the 'rectangle' at the right end of the above plot. On the obtained histogram, shown below, an exponential decay was observed with a very short time constant of 2 ms and a significant amplitude of  $6 \cdot 10^{-5}$  hits per second. Seeing that the rate of correlated pairs is only of 124.4/day when the reactor is off (and should stay in the same order of magnitude with the new cuts) it seems to me unlikely that very high-energy signals can simulate stopping muons such that the frequency of triple correlations reaches 500 Hz. Therefore I think it might be slightly more likely that this exponential decay is due to the electronics in the acquisition.





Not to be perturbed by this background, a lower  $\Delta t$  bound was set at 0.01s, which is very small compared to the time constant of  ${}^9\text{Li}$  decay (0.27 s) and at five time constants for this exponentially decaying background signal.



The top right histogram above shows the distribution against  $\Delta t$  below 0.01s, this time for an energy minimum at 1600 MeV. The three next are plots of the number of events vs  $\Delta t$  over 25s, with three successive minimal energies set at 1600 MeV, 2000 MeV and 3000 MeV. It can be observed from the first histogram that the same sharp exponential decay can be observed, with a similar time constant around 2 ms. This can be indicative as to the cause of the appearance of this pattern.

From other plots, no clear exponential decay is observable over the statistical fluctuation of the accidental background. Therefore only a higher bound can be given to the number of  ${}^9\text{Li}$  events per day. The mean number of accidentals was estimated for  $\Delta t = 2\text{s}$  to  $\Delta t = 25\text{s}$  not to include any potential  ${}^9\text{Li}$  signal. For the  ${}^9\text{Li}$  exponential decay to be visible among the statistical fluctuation in the distribution of  ${}^9\text{Li}$  events and that of accidental events, the total number of  ${}^9\text{Li}$  events must verify the inequality:

$$N_{Li} > \sqrt{N_{Li} + N_{acc}}$$

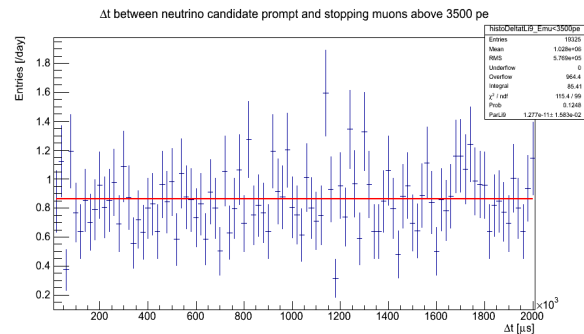
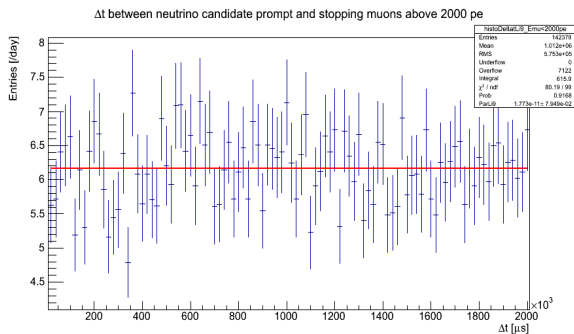
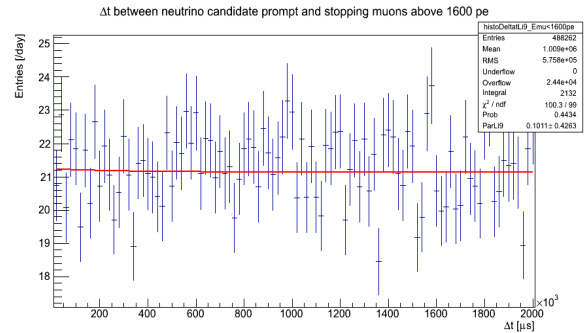
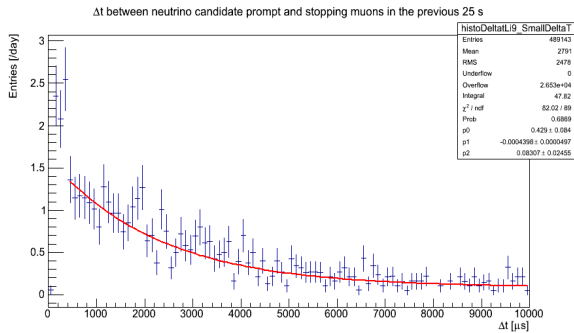
Or equivalently, solving the quadratic inequation:

$$N_{Li} > \frac{1 + \sqrt{1 + 4N_{acc} \text{AnalysisTime}}}{2 \text{AnalysisTime}}$$

As all first bin contents were within  $1 \sigma$  of the accidental background level, I estimated a maximal value for the number of  ${}^9\text{Li}$  events in the first bin at  $3 \sigma$  ie at 99.7% confidence level. The bin width (0.25 s) being approximately equal to the  ${}^9\text{Li}$  decay time constant, the content of the first bin would include 63% of the integral  ${}^9\text{Li}$  signal. Because of the lack of a clearly observable signal it is difficult to know the amount of  ${}^9\text{Li}$  events rejected by each muon energy cut. Results are summarised below.

Stopping Muon Energy (MeV)	Mean nb of accidentals (/bin/day)	Error in the mean (/bin/day)	Sigma (in acc bkgd in the 2 first s) (/bin/day)	1st bin content within (in nb of sigma)	63% Nmax (/day) at 3 sigma (C.L.=99.7%)	Nmax (/day)
1600	267.0	0.4	3.93	1	11.79	18.71429
2000	77.8	0.2	2.14	1	6.42	10.19048
3500	10.91	0.08	0.81	1	2.43	3.857143

Over the first 2s, the obtained distribution with a decaying exponential with  ${}^9\text{Li}$ 's lifetime and imposing the amount of accidentals to that found above as well as the amount of  ${}^9\text{Li}$  to be positive. What is observed is coherent with a flat fit.



The higher bounds evaluated for the number of  ${}^9\text{Li}$  events are compatible with the extrapolation from DCHOOZ results, without allowing us to have a more precise idea of the number of  ${}^9\text{Li}$  events per day in Nucifer. The only clear conclusion that can be drawn is that the  ${}^9\text{Li}$  background is not significant compared to the accidental noise and its fluctuation in this experiment.

## D) Conclusions

Taking part exclusively and intrinsically in nuclear interactions, neutrinos may present key applications in nuclear reactor and non-proliferation monitoring. Moreover, with the recently observed reactor neutrino anomaly, the eventuality of a fourth neutrino, at the limit of the Standard Model, could contribute to the understanding of the mysteries of dark matter or of the lack of antimatter in the universe. As a potential contributor to both major applied and fundamental questions, the Nucifer experiment consists in the installation of a liquid scintillator antineutrino detector from commercial components near the experimental Osiris reactor in Sacaly. Because it is very close to the core (only 7 m away) and the Earth surface (11 m beneath the reactor pool) accidental and correlated backgrounds due to the reactor core (neutrons, $\gamma$ ) or cosmic particles (muons, $\gamma$ ) are very important compared to the amount of neutrinos detected. Therefore understanding the different sources of background and optimising the amounts of signal and noise included can be determinant for the experiment.

A first part of the internship work consisted in optimising energy,  $\Delta t$  and PSD ranges to discriminate neutrino signals, in order to reject as much background as possible and include as much signal as possible. The optimised cuts were opened overall, with more significant changes for the delayed signal lower energy bound compared to nominal cuts. The prompt energy is now included **between 2.01 MeV and 7.13 MeV**, the delayed energy **between 4.18 MeV and 9.59 MeV** and the time between the two signals **below 40  $\mu$ s**. The PSD cut was changed from a horizontal to a sloping line in the  $Q_{tail}/Q_{tot}$  vs  $Q_{tot}$  plot, from the point **(680pe, 0.269)** to the point **(2720pe, 0.233)**. The results was conclusive, yielding an increase of **13% in the optimisation's FoM** upon re-analysis over existing data. The surprising shape of the delayed signal energy distribution was also mostly rectified thanks to the rejection of more recoil proton background for the higher energies.

A study on the  ${}^9\text{Li}$  correlated background was also performed during the internship, comparing an extrapolation from a DC power law with analysis from Nucifer data. Re-scaling with the mean muon energy, the mean muon flux, the number of carbon nuclei in the scintillator and the muon veto life time, between **1.36 evts/day** and **2.72 evts/day** were expected in Nucifer. For our experiment the analysis was undertaken lowering the gain of one PMT in order to tag only stopping muons and look for correlations between these and neutrino candidates. Plotting the number of triple correlations vs the time between the stopping muon event and the prompt signal, the  ${}^9\text{Li}$  radioactive exponential decay, of lifetime 0.27 s was not apparent among accidental background statistical fluctuation. Therefore several potential higher bounds for the number of  ${}^9\text{Li}$  events were determined, all consistent with the DC extrapolation. It can simply be concluded that  ${}^9\text{Li}$  is not a major source of background noise in Nucifer.

Questions that remain are the shape of the PSD plot, which is similar for different scintillating liquids or experimental setups, as well as the 2 ms time constant exponential decay observed in the search for  ${}^9\text{Li}$  candidates. While the first point most certainly raises physical implications, the second may highlight an error in the analysis codes, a dysfunction of the apparatus and electronics or potentially other physical phenomena.

## **E) References**

- [1] A. Bernstein, G. Baldwin, B. Boyer, M. Goodman, J. Learned, J. Lund, D. Reyna, R. Svoboda, “Nuclear Security Applications of Antineutrino Detectors: Current Capabilities and Future Prospects”. pp 127-192, Science & Global Security Volume 18, Issue 3, 2010.
- [2] J. Gaffiot, “Étude des neutrinos de réacteur : mise en place et caractérisation du détecteur Nucifer”. PhD Thesis, Université Paris Sud, 2012.
- [3] Official ROOT website <http://root.cern.ch/drupal/>
- [4] Liangjian Wen, Jun Cao, Kam-Biu Luk, Yuqian Ma, Yifang Wang, Changgen Yang, “Measuring cosmogenic  $^9\text{Li}$  background in a reactor neutrino experiment”. Nucl.Instrum.Meth. A564, 471-474, 2006.
- [5] Y. Abe et al. [Double Chooz Collaboration] “Direct Measurement of Backgrounds using Reactor-Off Data in Double Chooz”. Phys. Rev. D 87, 011102, 2013.

## **F) Appendix**

### **Appendix 1: Macro examples**

#### Optimisation of the energy and $\Delta t$ cuts for different amounts of accidental noise

```
#include <TROOT.h>
#include <TFile.h>
#include <TH3.h>
#include <TCanvas.h>
#include <TPad.h>
#include <Riostream.h>

const double CalibFactor = 340;
const double Tau = 24.6;

//Reactor OFF
const double IntPromptRefOff = 3416.35; // 2<Ep<6
const double IntDelayedRefOff = 3327.85; //6<Ed<10
const double IntDeltatOffRef = 16.6168; //5<Deltat<45
const double NCosmicRef = 124.4; //above ref cuts

//Simulation
const double IntPromptSimRef = 1.55477e+06; // 2<Ep<6
const double IntDelayedSimRef = 691524; // 6<Ed<10
const double NSignalRef = 137; //above ref cuts

//Accidental
const double IntPromptBRef = 8.14952e+06; // above ref cuts
const double IntDelayedBRef = 710405; // above ref cuts
const double a = 10; //number of false delayed candidates taken for each
prompt

const double tminref = 5;
const double tmaxref = 45;

void SignalIntegral(double NBruitRef = 4000, /*double EPmin = 2, */double
EPmax = 7.13, /*double EDmin = 6, */double EDmax = 9.59, double tmin = 5/*,
double tmax = 45*/)
{
double C = 1/Tau/(exp(-tminref/Tau)-exp(-tmaxref/Tau));
//Noise from reactor-OFF measurements
//Prompt
TFile *f = new TFile("20jrs_PSD_OFF.root");//with veto and PSD
TH1F *hPrompt = (TH1F *)f->Get("histoPrompt");

//Noise for E<2MeV, extrapolating from fit
TH1F *hfit = (TH1F *)gROOT->FindObject("histofit");
if (hfit){
hfit->Reset();
}
}
```

```

else {
    hfit = new TH1F ("histofit","Fit_Signal_OFF",100,0.,680);
}

for (Double_t x=0;x<680;x++)
{
    Double_t fx = 1.81447e+02-2.34323e-01*x+9.62864e-05*x*x;
    hfit->Fill(x,fx);
}

//Delayed
// TH1F *hDelayed = (TH1F *)f->Get("histoDelayed");

//Signal from Simulation
TFile *fSim = new TFile("Analyzer_QTInucut_Neutrinos.00-64.root");
//Prompt
TH1F *hPromptSim = (TH1F *)fSim->Get("SimuAlgoDir/nQtot_prompt");
//Delayed
TH1F *hDelayedSim = (TH1F *)fSim->Get("SimuAlgoDir/nQtot_delayed");

//Noise from reactor-ON measurements
TFile *fB = new TFile("Analyzer_QTbary_nucut_nuco_Run2013143-13959-13996.root");
TH1F *hBruit = (TH1F *)fB->Get("QtotAlgoDir/nQtot");

TH3F *h = new TH3F("histo","FoM vs tmax vs Eadmin vs EPmin",11,1.45,2.55,21,3.95,6.05,31,29.5,60.5);
// hEPmintmax->Draw("SURF");

for (Double_t tmax=40;tmax<61;tmax+=1)
{
    for (Double_t Eadmin=4.0;Eadmin<6.1;Eadmin+=0.1)
    {
        for (Double_t EPmin=1.5;EPmin<2.6;EPmin+=0.1)
        {
            // cout<<"\n Eadmin = "<<Eadmin<<endl;
// Reactor OFF
            Double_t IntPromptOff = hPrompt->Integral(hPrompt->FindBin(2*CalibFactor),hPrompt->FindBin(EPmax*CalibFactor),"")+hfit->Integral(hfit->FindBin(EPmin*CalibFactor),hfit->FindBin(2*CalibFactor),"");
            Double_t Fp = IntPromptOff/IntPromptRefOff;

            Double_t IntDelayedOff = hDelayedSim->Integral(hDelayedSim->FindBin(Eadmin*CalibFactor),hDelayedSim->FindBin(EDmax*CalibFactor),"");
            /*taken from the simulation that superposes well with the data, to get Eadmin down to 4MeV*/
            Double_t Fd = IntDelayedOff/IntDelayedSimRef;

```

```

    Double_t FDeltat = C* Tau*(exp(-tmin/Tau)-exp(-tmax/Tau));

    Double_t NCosmic = NCosmicRef*Fp*Fd*FDeltat;
    //    cout<<"NCosmic = "<<NCosmic<<endl;

    // Signal from Simulation
    Double_t IntPromptSim = hPromptSim->Integral(hPromptSim-
>FindBin(EPmin*CalibFactor),hPromptSim->FindBin(EPmax*CalibFactor),"");
    Double_t Fpsim = IntPromptSim/IntPromptSimRef;

    Double_t IntDelayedSim = hDelayedSim->Integral(hDelayedSim-
>FindBin(EDmin*CalibFactor),hDelayedSim->FindBin(EDmax*CalibFactor),"");
    Double_t Fdsim = IntDelayedSim/IntDelayedSimRef;

    //Double_t FDeltatOn = hDeltatexp->Integral(hDeltatexp-
>FindBin(tmin),hDeltatexp->FindBin(tmax),"");
    // FDeltatOn is same as for the OFF case

    Double_t NSignal = NSignalRef*Fpsim*Fdsim*FDeltat;
    //    cout<<"NSignal = "<<NSignal<<endl;

    // Noise from reactor ON
    Double_t IntPromptB = hBruit->Integral(hBruit-
>FindBin(EPmin*CalibFactor),hBruit->FindBin(EPmax*CalibFactor),"");
    Double_t Fpb = IntPromptB/IntPromptBRef;

    Double_t IntDelayedB = hBruit->Integral(hBruit-
>FindBin(EDmin*CalibFactor),hBruit->FindBin(EDmax*CalibFactor),"");
    Double_t Fdb = IntDelayedB/IntDelayedBRef;

    Double_t FDeltatB = (tmax-tmin)/(tmaxref-tminref);
    Double_t NBruitON = NBruitRef*Fpb*Fdb*FDeltatB;
    //    cout<<"NBruit = "<<NBruitON<<endl;

    Double_t FoM = NSignal/sqrt(NSignal+2*NCosmic+(1+1/a)*NBruitON);
    //    cout<<"FoM = "<<FoM<<endl;

    h->Fill(EPmin,EDmin,tmax,FoM);
    cout<<"\n EPmin = "<<EPmin<<endl;
    cout<<"EPmax = "<<EPmax<<endl;
    cout<<"EDmin = "<<EDmin<<endl;
    cout<<"EDmax = "<<EDmax<<endl;
    cout<<"tmax = "<<tmax<<endl;
    cout<<"FoM"<<FoM<<endl;
    }
}
}
cout<<"Noise = "<<NBruitRef<<endl;
Double_t Max = h->GetMaximum();
cout<<"global max = "<<Max<<endl;

Int_t locmaxx,locmaxy,locmaxz;
h->GetMaximumBin(locmaxx,locmaxy,locmaxz);

```

```

double MaxX = h->GetXaxis()->GetBinCenter(locmaxx);
cout<<"EPmin = "<<MaxX<<endl;
double MaxY= h->GetYaxis()->GetBinCenter(locmaxy);
cout<<"EDmin = "<<MaxY<<endl;
double MaxZ= h->GetZaxis()->GetBinCenter(locmaxz);
cout<<"tmax = "<<MaxZ<<endl;

//   TFile *f = new TFile("CutsVariation.root", "UPDATE");
//   hEPmintmax->Write();
//   delete f;

    f->Close();
    fSim->Close();
    fB->Close();
}

```

### Optimisation of the PSD cut

```

#include <TROOT.h>
#include <TFile.h>
#include <TH1.h>
#include <TH2.h>
#include <TCutG.h>
#include <TCanvas.h>
#include <TPad.h>
#include <Riostream.h>

Double_t NormON = 5653; // integral in the region 0.29<Qtail/Qtot<0.4
Double_t NormOFF = 1.265e+04; // integral in the region 0.29<Qtail/Qtot<0.4

const double NnuON = 138;
const double FracAccNu = 15.47;//Fraction of accidentals to neutrinos
const double NOFF = 124.4;
    //From MergeSummary

Double_t w = 10; // Number of uncorrelated windows opened to measure the
amount of accidental background

void Test1()
{
    // Getting histograms for reactor-ON accidentals and reactor-OFF all and
accidentals
    // Same time periods for all reactor-ON hists and all reactor-OFF ones
    TFile *fAccON = new TFile("PSD_Acc_ON.root");
    TH2F *hAccON = (TH2F *)fAccON->Get("histoPrompt");
    //   hAccON->Scale(NnuON*FracAccNu/hAccON->Integral()); //Normalised to
number of acc events per day (reac on)

    TFile *fOFF = new TFile("PSD_OFF.root");
    TH2F *hOFF = (TH2F *)fOFF->Get("histoCorr");
    TH2F *hAccOFF = (TH2F *)fOFF->Get("histoAcc");
}

```



```

    TH2F *hCorrOFF = (TH2F *)hOFF->Clone();
    hCorrOFF->Add(hOFF,hAccOFF,1,-1);
//    hCorrOFF->Scale(NOFF/hCorrOFF->Integral()); //Normalised to number of
cosmic particle events per day (reac off)

//    //Outline of neutrino signal
//    TFile *fCorrON = new TFile("PSD_Corr_ON.root");
//    TH2F *hON = (TH2F *)fCorrON->Get("histoPrompt");
//    TH2F *hNu = (TH2F *)hON->Clone();
//    hNu->Add(hON,hAccON,1,-1);
//

TCutG *cutg = new TCutG("cut",4);
cutg->SetVarX("y");
cutg->SetVarY("x");

    Double_t SsurDeltaSmax = 0;
    Double_t amax = 0;
    Double_t bmax = 0;
//    Double_t cmax = 0;
//    Double_t dmax = 0;

    for (Double_t a=0.22;a<0.251;a+=0.001)
    {
        for (Double_t b=0.265;b<0.301;b+=0.001)
        {
//            for (Double_t c=0.24;c<0.271;c+=0.001)
//            {
//                for (Double_t d=700;d<1000;d+=10)
//                {
                    cutg->SetPoint(0,680.,0);
                    cutg->SetPoint(1,680.,b);
//                    cutg->SetPoint(2,d,c);
                    cutg->SetPoint(2,2720.,a);
                    cutg->SetPoint(3,2720.,0);
                    cutg->SetPoint(4,680.,0);

                    // signal (ie neutrinos) approximated to accidentals (ie gammas from
reac tor) because of their similar Qtail/Qtot signal shape and the large
amount of data for accidentals
                    // noise approximated for correlated reactor-OFF data
                    Double_t Signal = cutg->IntegralHist(hAccON,"");
                    Double_t DeltaS = sqrt(hAccON->Integral()/hAccON->Integral()*cutg-
>IntegralHist(hAccON,"")*(1+1/w+1/FracAccNu/FracAccNu)+cutg-
>IntegralHist(hCorrOFF,"")*(1+NnuON/NOFF));
                    Double_t SsurDeltaS = Signal/DeltaS;

                    if (SsurDeltaS>SsurDeltaSmax) {
//                        cutg->Draw();
                        SsurDeltaSmax = SsurDeltaS;

```

```

    amax = a;
    bmax = b;
//    cmax = c;
//    dmax = d;

}

cout<<a<<"\t"<<b<<"\t"/*<<c<<"\t"<<d<<"\t"*/<<SsurDeltaS<<"\t"<<SsurDeltaSm
ax<<endl;
    }
    }
//    }
//    }
    hAccON->Scale(NnuON*FracAccNu/hAccON->Integral()); //Normalised to number
of acc events per day (reac on)
    hAccON->Draw();

    cout<<"S/DeltaS = "<<SsurDeltaSmax<<endl;
    cout<<"a = "<<amax<<endl;
    cout<<"b = "<<bmax<<endl;
//    cout<<"c = "<<cmax<<endl;
//    cout<<"d = "<<dmax<<endl;
//
    delete cutg;

    TCutG *cutgmax = new TCutG("optimalcut",4);
    cutgmax->SetVarX("y");
    cutgmax->SetVarY("x");
    cutgmax->SetPoint(0,680.,0);
    cutgmax->SetPoint(1,680.,bmax);
//    cutgmax->SetPoint(2,dmax,cmax);
    cutgmax->SetPoint(2,2720.,amax);
    cutgmax->SetPoint(3,2720.,0);
    cutgmax->SetPoint(4,680.,0);
    cutgmax->Draw();

    // Estimate of the fraction of neutrinos included in the cut
    Double_t FNu = cutgmax->IntegralHist(hAccON,"")/hAccON->Integral();
    Double_t FB = cutgmax->IntegralHist(hCorrOFF,"")/hCorrOFF->Integral();

    cout<<"Fraction of neutrino signal included = "<<FNu<<endl;
    cout<<"Fraction of reactor-off background included = "<<FB<<endl;

}

```

### Simulation of muons crossing the Nucifer liquid to find the mean distance travelled through the liquid

```

#include <TROOT.h>
#include <TMath.h>
#include <TFile.h>
#include <TH1.h>
#include <TH2.h>
#include <TF1.h>

```

```

#include <TRandom3.h>
#include <TCutG.h>
#include <TCanvas.h>
#include <TPad.h>
#include <Riostream.h>

Double_t h = 0.73; //detector height (ie liquid height)
Double_t R = 0.60; //detector radius

Double_t DistanceToZAxis(Double_t *z, Double_t *par)
{
    Double_t t = (z[0]-par[4])/par[5];
    Double_t x = par[0]+par[1]*t;
    Double_t y = par[2]+par[3]*t;
    Double_t distZ = sqrt(x*x+y*y);
    return distZ;
}

void Muon(Int_t nbmumax = 1e+09)
{
    TH1F *hdist = new TH1F ("histodist","distribution of the distance
travelled by muons in the detector",151,0.,1.50);
    hdist->Draw();
    hdist->Draw("hist same c");

    TH2F *hxy = new TH2F("histoXY","xy distribution of muons that travel
through the detector",100,-5.,5.,100,-5.,5.);
    TH1F *hphi = new TH1F("histophi","Phi distribution of muons that travek
through the detector",100,0.,2*TMath::Pi());
    TH1F *htheta = new TH1F("histotheta","Theta distribution of muons that
travek through the detector",100,0.5*TMath::Pi(),1.5*TMath::Pi());

    // TF1 *unifdistrpt = new TF1("const","1.",-1.,1.);
    // TF1 *unifdistrphi = new TF1("const","1.",0.,1.);
    TF1 *proba = new
TF1("proba","cos(x)*cos(x)",0.5*TMath::Pi(),1.5*TMath::Pi());

    // Creating a Root function based on function DistanceToZAxis above
    TF1 *func = new TF1("DistanceToZAxis",DistanceToZAxis,0.,h,6);
    Double_t squareside = 5.;
    Double_t x1 = 0.;
    Double_t y1 = 0.;
    Double_t x2 = 0.;
    Double_t y2 = 0.;
    Double_t z1 = 0.;
    Double_t z2 = 0.;

    Int_t i = 0; // total distance the muons go through in the liquid
    Double_t dtot = 0.;
    Double_t deltadtotsq = 0.;

```

```

TRandom3 *random = new TRandom3();
random->SetSeed(0);
for (Int_t nbmu=0;nbmu<=nbmumax;nbmu++)
{
    cout<<"number of muons = "<<nbmu<<endl;
    // Random muon 'start points' on a virtual plane hovering 3m above the
detector bottom
    double a0 = random->Uniform(-squareside,squareside);
    double b0 = random->Uniform(-squareside,squareside);
    double c0 = 0.75;

    // Random muon trajectory phi and theta angles

    double phi = random->Uniform(0,2*TMath::Pi());

    double theta = proba->GetRandom();

    hphi->Fill(phi);
    htheta->Fill(theta);
    // Converts angles into cartesian line vector coordinates
    Double_t a = sin(theta)*cos(phi);
    Double_t b = sin(theta)*sin(phi);
    Double_t c = cos(theta);

//      cout<<"phi = "<<phi<<"\t theta = "<<theta<<"\t a0 = "<<a0<<"\t b0
= "<<b0<<endl;

    // Setting initial values and parameter names
    func->SetParameters(a0,a,b0,b,c0,c);

    // Considering the detector as a stack of thin cylindrical slices. A
muon that travels through the detector enters through one slice and exits
through another.
    for (Double_t zmax=h;zmax>0;zmax+!=-0.01)
    {
        if (func->Eval(zmax)<=R)
        {
            //      cout<<"zmax = "<<zmax<<endl;
            x1 = a0+a*(zmax-c0)/c;
            y1 = b0+b*(zmax-c0)/c;
            hxy->Fill(a0,b0);
            z1 = zmax;
            zmax=0;

            for (Double_t zmin=0;zmin<z1;zmin+=0.01)
            {
                if (func->Eval(zmin)<=R)
                {
//      cout<<"zmin = "<<zmin<<endl;
                x2 = a0+a*(zmin-c0)/c;
                y2 = b0+b*(zmin-c0)/c;
                z2 = zmin;

```

```

        Double_t d = sqrt((x2-x1)*(x2-x1)+(y2-y1)*(y2-y1)+(z2-z1)*(z2-z1));
        Double_t deltad = 0.01*sqrt(2*(a*a+b*b+c*c))/c; // error in d
        hdist->Fill(d);
        hdist->SetBinError(hdist->FindBin(d),deltad);
//      gPad->Modified();gPad->Update();
        dtot = dtot + d;
        deltadtotsq = deltadtotsq + deltad*deltad; // square of the error
in the total (summed) distance
        i++;
        zmin=h;

    }
}
}
}

    cout<<"number of muons crossing detector = "<<i<<endl;
    cout<<"dtot = "<<dtot<<endl;

}

TFile *fout = new TFile("SimMu2.root","recreate");
hdist->Write();
hxy->Write();
hphi->Write();
htheta->Write();
fout->Close();
delete fout;
Double_t dmean = dtot/i;
Double_t deltadmean = sqrt(deltadtotsq)/i;
cout<<"mean distance crossed by muons = " <<dmean<<endl;
cout<<"error in the mean = " <<deltadmean<<endl;
cout<<hdist->GetMean()<<endl;
}

```

### Adding histograms from a list of analyzer files and saving into a ROOT file

```

#include <TROOT.h>
#include <TMath.h>
#include <TFile.h>
#include <TH1.h>
#include <TH2.h>
#include <TF1.h>
#include <TRandom3.h>
#include <TCutG.h>
#include <TCanvas.h>
#include <TPad.h>
#include <Riostream.h>

const int NFilesON = 15;// number of ON analyzers

TString FileNamesON[NFilesON] = {
"Analyzer_QTnucut_Run2013088-12153-12233.root",

```

```

"Analyzer_QTnucut_Run2013094-12394-12473.root",
"Analyzer_QTnucut_Run2013099-12555-12634.root",
"Analyzer_QTnucut_Run2013101-12635-12716.root",
"Analyzer_QTnucut_Run2013105-12812-12892.root",
"Analyzer_QTnucut_Run2013110-12973-13052.root",
"Analyzer_QTnucut_Run2013112-13053-13335.root",
"Analyzer_QTnucut_Run2013123-13336-13415.root",
"Analyzer_QTnucut_Run2013125-13416-13495.root",
"Analyzer_QTnucut_Run2013130-13576-13687.root",
"Analyzer_QTnucut_Run2013134-13688-13789.root",
"Analyzer_QTnucut_Run2013138-13790-13869.root",
"Analyzer_QTnucut_Run2013140-13870-13949.root",
"Analyzer_QTnucut_Run2013142-13950-14035.root",
"Analyzer_QTnucut_Run2013145-14036-14105.root"

};

const int NFilesOFF = 4;
TString FileNamesOFF[NFilesOFF] = {
"Analyzer_QTnucut_Run2013081-11911-14182.root",
"Analyzer_QTnucut_Run2013150-14184-14548.root",
"Analyzer_QTnucut_Run2013164-14549-14881.root",
"Analyzer_QTnucut_Run2013177-14882-15567.root"
};

void ReadFiles()
{
    // All reference histograms are with veto, R<650
    // Reactor-ON
    // Qtot plots
    TH1F *hCorrPrptON=0;
    TH1F *hPON[NFilesON];
    TH1F *hCorrDlydON=0;
    TH1F *hDON[NFilesON];

    // PSD (Qtail/Qtot vs Qtot) plots
    TH2F *hCorrON=0;
    TH2F *hCON[NFilesON];
    TH2F *hAccON=0;
    TH2F *hAON[NFilesON];

    TFile* filesON[NFilesON];

    // Reactor-OFF
    // Qtot plots
    TH1F *hCorrPrptOFF=0;
    TH1F *hPOFF[NFilesOFF];
    TH1F *hCorrDlydOFF=0;
    TH1F *hDOFF[NFilesOFF];

    // PSD (Qtail/Qtot vs Qtot) plots
    TH2F *hCorrOFF=0;
    TH2F *hCOFF[NFilesOFF];

```

```

TH2F *hAccOFF=0;
TH2F *hAOFF[NFilesOFF];

TFile* filesOFF[NFilesOFF];

// Reading Files ON
for (int i=0; i<NFilesON; i++) {
    TString CurrentNameON = "../RUNS_NEWCUTS/DATA_ON/";
    CurrentNameON += FileNamesON[i].Data();
    cout << CurrentNameON.Data() << endl;
    filesON[i] = new TFile(CurrentNameON.Data(),"READ");
    hPON[i] = new TH1F();
    hDON[i] = new TH1F();
    hCON[i] = new TH2F();
    hAON[i] = new TH2F();

    filesON[i]-
>GetObject("NeutrinoCutAlgoDir/Qtot__Veto&PSD_R<650/hQtot_CorrPrpt_2.0<Ep<7
.1_4.2<Ed<9.6_Veto&PSD_R<650",hPON[i]);
    filesON[i]-
>GetObject("NeutrinoCutAlgoDir/Qtot__Veto&PSD_R<650/hQtot_CorrDlyd_2.0<Ep<7
.1_4.2<Ed<9.6_Veto&PSD_R<650",hDON[i]);
    filesON[i]-
>GetObject("NeutrinoCutAlgoDir/QQ_Qtot__Veto_R<650/hQQ_Qtot_2.0<Ep<7.1_4.2<
Ed<9.6_Veto_R<650",hCON[i]);
    filesON[i]-
>GetObject("NeutrinoCutAlgoDir/QQ_Qtot__Veto_R<650/hQQ_Qtot_Acc_2.0<Ep<7.1_
4.2<Ed<9.6_Veto_R<650",hAON[i]);

    if (i==0) {
        hCorrPrptON=(TH1F*)hPON[i]->Clone();
        hCorrDlydON=(TH1F*)hDON[i]->Clone();
        hCorrON=(TH2F *)hCON[i]->Clone();
        hAccON=(TH2F *)hAON[i]->Clone();
    }
    else {
        hCorrPrptON->Add(hPON[i]);
        hCorrDlydON->Add(hDON[i]);
        hCorrON->Add(hCON[i]);
        hAccON->Add(hAON[i]);
    }
    cout << "i = " << i <<endl;
}

// Reading Files OFF
for (int j=0; j<NFilesOFF; j++) {
    TString CurrentNameOFF = "../RUNS_NEWCUTS/DATA_OFF/";
    CurrentNameOFF += FileNamesOFF[j].Data();
    cout << CurrentNameOFF.Data() << endl;
    filesOFF[j] = new TFile(CurrentNameOFF.Data(),"READ");
    hPOFF[j] = new TH1F();
    hDOFF[j] = new TH1F();
}

```

```

    hCOFF[j] = new TH2F();
    hAOFF[j] = new TH2F();

    filesOFF[j]-
>GetObject("NeutrinoCutAlgoDir/Qtot__Veto&PSD_R<650/hQtot_CorrPrpt_2.0<Ep<7
.1_4.2<Ed<9.6_Veto&PSD_R<650",hPOFF[j]);
    filesOFF[j]-
>GetObject("NeutrinoCutAlgoDir/Qtot__Veto&PSD_R<650/hQtot_CorrDlyd_2.0<Ep<7
.1_4.2<Ed<9.6_Veto&PSD_R<650",hDOFF[j]);
    filesOFF[j]-
>GetObject("NeutrinoCutAlgoDir/QQ_Qtot__Veto_R<650/hQQ_Qtot_2.0<Ep<7.1_4.2<
Ed<9.6_Veto_R<650",hCOFF[j]);
    filesOFF[j]-
>GetObject("NeutrinoCutAlgoDir/QQ_Qtot__Veto_R<650/hQQ_Qtot_Acc_2.0<Ep<7.1_
4.2<Ed<9.6_Veto_R<650",hAOFF[j]);

    if (j==0) {
        hCorrPrptOFF=(TH1F*)hPOFF[j]->Clone();
        hCorrDlydOFF=(TH1F*)hDOFF[j]->Clone();
        hCorrOFF=(TH2F *)hCOFF[j]->Clone();
        hAccOFF=(TH2F *)hAOFF[j]->Clone();
    }
    else {
        hCorrPrptOFF->Add(hPOFF[j]);
        hCorrDlydOFF->Add(hDOFF[j]);
        hCorrOFF->Add(hCOFF[j]);
        hAccOFF->Add(hAOFF[j]);
    }
    cout << "j = " << j <<endl;
}

hCorrPrptON->SetName("histoCorrPrptON");
hCorrDlydON->SetName("histoCorrDlydON");
hCorrON->SetName("histoCorrON");
hAccON->SetName("histoAccON");

hCorrPrptOFF->SetName("histoCorrPrptOFF");
hCorrDlydOFF->SetName("histoCorrDlydOFF");
hCorrOFF->SetName("histoCorrOFF");
hAccOFF->SetName("histoAccOFF");

TFile f_out("ANALYSIS_NEWCUTS.root","recreate");
f_out.cd();
hCorrPrptON->Write();
hCorrPrptOFF->Write();
hCorrDlydON->Write();
hCorrDlydOFF->Write();
hCorrON->Write();
hCorrOFF->Write();
hAccON->Write();
hAccOFF->Write();
f_out.Close();

```



}

## Appendix 2: Error propagation

Estimating errors is a key part in signal detection physics. In order to deduce from measurements the characteristics of the neutrino signal, one must be able to extract it from the accidental background and its uncertainty. Data being usually presented under the shape of histograms, each bin contains a certain number of hits. By definition the statistical error is the square root of this number of hits. (Intuitively, for each hit counted the error can reach  $\pm 1$  hit. If each error is materialised by a vector of unit length, that can any direction - like the imprecision when measuring a length with a rule - and all vectors are added on ends of each other, with a random walk model the root mean square distance between the two ends, or mean error is the square root of the number of vectors. As the amount of data increases and the number of hits grows, the relative statistical error drops.) When a histogram is re-scaled by a factor  $\alpha$ , for example by the analysis time or by the number of shifted gates opened for accidentals, the relative error must be conserved.

$$\frac{\delta N_{Tot}}{N_{Tot}} = \frac{\delta N_{Hist}}{N_{Hist}}$$

$$\therefore \delta N_{Hist} = \frac{\delta N_{Tot} N_{Hist}}{N_{Tot}} = \frac{\delta N_{Tot}}{\alpha} = \frac{\sqrt{N_{Tot}}}{\alpha} = \sqrt{\frac{N_{Hist}}{\alpha}}$$

Using this result, and other basic error propagation rules for addition and multiplication, most histogram error bars and  $S/\delta S$  FoMs can be derived. Inherently to the nature of histograms, the sum of the number of hits in a certain range is equal to the integral over the bins in the range. A perhaps slightly subtle example of such an error propagation is given below, for the FoM of the PSD cut optimisation, because the distribution of neutrino candidates is approximated using the accidental spectra:

$$N_{Tot} = N_v + N_{Acc} + N_{off} * \frac{NormON}{NormOFF}$$

Where  $N_{Tot}$  is the total number of hits measured,  $N_v$  and  $N_{Acc}$  are estimated from the same runs and  $NormON$  and  $NormOFF$  are the typical integrals in the recoil proton region for reactor-on and reactor-off data (time normalisation can show the risk of including corrupt runs where the analysis time has been recorded but no data was taken).

$$\therefore \delta N_v = \sqrt{N_{Tot} + \frac{N_{Acc}}{w} + N_{off} * \frac{NormON}{NormOFF}}$$

with  $w$  the number of shifted time windows opened in search for accidentals. Substituting the expression for  $N_{Tot}$  back in:

$$\therefore \delta N_v = \sqrt{N_v + \left(1 + \frac{1}{w}\right) N_{Acc} + \left(1 + \frac{NormON}{NormOFF}\right) N_{off}}$$

Using  $N_v = f * N_{Acc}$

$$\therefore \delta N_v = \sqrt{\left(1 + f\left(1 + \frac{1}{w}\right)\right) N_{Acc} + \left(1 + \frac{NormON}{NormOFF}\right) N_{off}}$$